THE JOURNAL OF BIOLOGICAL CHEMISTRY
Vol. 279, No. 19, Issue of May 7, pp. 19691–19697, 2004
Printed in U.S.A.

Cdt1 Phosphorylation by Cyclin A-dependent Kinases Negatively Regulates Its Function without Affecting Geminin Binding*

Received for publication, December 3, 2003, and in revised form, February 18, 2004
Published, JBC Papers in Press, March 1, 2004, DOI 10.1074/jbc.M313175200

Nozomi Sugimoto‡§, Yasutoshi Tatsumi‡, Tatsuya Tsurumi¶, Akio Matsukage§, Tohru Kiyono‡, Hideo Nishitani‖, and Masatoshi Fujita‡**

From the ‡Virology Division, National Cancer Center Research Institute, 5-1-1 Tsukiji, Chuohku, Tokyo 104-0045, the ¶Division of Virology, Aichi Cancer Center Research Institute, 1-1 Kanokoden, Chikusa-ku, Nagoya 464-8681, the §Faculty of Science, Japan Women's University, 2-8-1 Mejirodai, Bunkyouku, Tokyo 112-8679, and the ‖Department of Molecular Biology, Graduate School of Medical Science, Kyushu University, Maidashi 3-1-1, Higashiku, Fukuoka 812-8582, Japan

The current concept regarding cell cycle regulation of DNA replication is that Cdt1, together with origin recognition complex and CDC6 proteins, constitutes the machinery that loads the minichromosome maintenance complex, a candidate replicative helicase, onto chromatin during the G_1 phase. The actions of origin recognition complex and CDC6 are suppressed through phosphorylation by cyclin-dependent kinases (Cdks) after S phase to prohibit rereplication. It has been suggested in metazoan cells that the function of Cdt1 is blocked through binding to an inhibitor protein, geminin. However, the functional relationship between the Cdt1-geminin system and Cdks remains to be clarified. In this report, we demonstrate that human Cdt1 is phosphorylated by cyclin A-dependent kinases dependent on its cyclin-binding motif. Cdk phosphorylation resulted in the binding of Cdt1 to the F-box protein Skp2 and subsequent degradation. In contrast, *in vitro* DNA binding activity of Cdt1 was inhibited by the phosphorylation. However, geminin binding to Cdt1 was not affected by the phosphorylation. Finally we provide evidence that inactivation of Cdk1 results in Cdt1 dephosphorylation and rebinding to chromatin in murine FT210 cells synchronized around the G_2/M phase. Taken together, these findings suggest that Cdt1 function is also negatively regulated by the Cdk phosphorylation independent of geminin binding.

Recent progress has uncovered molecular mechanisms by which DNA replication is cell cycle-controlled in eukaryotic cells (for reviews, see Refs. 1 and 2). The current concept is that a multiprotein complex, termed the prereplication complex (pre-RC),[1] is constructed during the G_1 phase based on origin recognition complex (ORC) binding to chromosomal DNA. CDC6 and Cdt1 proteins are recruited to the chromatin by interaction with ORC, and the resultant machinery may function as a loader for the MCM heterohexameric complex, which could function as a replicative helicase (3, 4). The mechanism seems basically conserved from yeast to metazoan cells, although it is more complicated in the latter (2).

Once cyclin-dependent kinases (Cdks) become active at the onset of S phase, pre-RC initiates replication accompanied by further assembly of multiple other proteins or protein complexes (1). Cdks physically interact with and phosphorylate ORC and CDC6 (5–10). However, considering that they are no longer necessary for initiation after loading MCMs (11, 12), such phosphorylation is unlikely to be involved in promotion of replication, although ORC and CDC6 could act as adapter molecules to tether Cdks to initiation sites. Prior to the DNA unwinding step, CDC45 is loaded onto chromatin, probably via physical interaction with the MCM complex (13–15). The loading is dependent on both Cdk and CDC7 kinase activities, and both these kinases phosphorylate the MCM complex (1, 13–15). However, it remains unclear how phosphorylation positively regulates this step. Once CDC45 is loaded, the DNA is unwound with the help of replication protein A (1).

To prevent rereplication, that is the reestablishment of pre-RC, rebinding of MCM needs to be suppressed during the S, G_2, and M phases of the cell cycle. Recent studies have suggested that Cdks also play a central role in this context. Thus, Cdk activity has a bipartite function in the regulation of DNA replication. The importance of Cdk1 kinase in mammals is clearly demonstrated by the fact that its inactivation results in rebinding of MCM proteins and subsequent rereplication (16, 17). Ablation of cyclin A, but not cyclin B, leads to rereplication in *Drosophila* tissue culture cells (18). Cdks prevent reestablishment of pre-RC through multiple redundant mechanisms (1, 2). One mechanism is by phosphorylation of CDC6, leading to degradation in yeast or nuclear export in mammalian cells (5–7, 19). In the latter situation, cyclin A-Cdk2 is one kinase responsible for this phosphorylation (6, 7). In human cells, ORC1 is degraded after S phase, presumably depending on phosphorylation by cyclin A-Cdk2 (10, 20). In budding yeast, the function of ORC2 is suppressed through Cdk phosphorylation (9). It has also been shown that the MCM complex is phosphorylated by Cdks (1, 2, 17). In budding yeast, it is necessary to block all three pathways for induction of rereplication without inhibiting Cdk activity (9). Also in mammalian cells, alteration of the regulation of the individual components alone, for example overexpression of the phosphorylation-deficient CDC6 mutant, fails to induce rereplication (6, 7).

In metazoans, geminin has been identified as another inhibitor of pre-RC formation (21), preventing the loading of MCM proteins by binding to and inhibiting Cdt1 (22–25). It appears after cells enter S phase and is destroyed during exit from

* This work was supported in part by grants from the Ministry of Education, Science, Sports, Culture, and Technology of Japan (to M. F. and H. N.), and from the Human Frontier Science Program Organization (to H. N.). The costs of publication of this article were defrayed in part by the payment of page charges. This article must therefore be hereby marked "*advertisement*" in accordance with 18 U.S.C. Section 1734 solely to indicate this fact.

** To whom correspondence should be addressed. Tel.: 81-3-3542-2511 (ext. 4702); Fax: 81-3-3543-2181; E-mail: mafujita@gan2.res.ncc.go.jp.

[1] The abbreviations used are: pre-RC, prereplication complex; ORC, origin recognition complex; Cdk, cyclin-dependent kinase; SCF, Skp1-Cdc53-F-box protein complex; GST, glutathione *S*-transferase; HA, hemagglutinin; DTT, dithiothreitol; MCM, minichromosome maintenance.

mitosis (21, 24). Contrary to the cyclin A case, reduction in the levels of geminin in *Drosophila* tissue culture cells results in partial, but not complete, rereplication (18). Therefore, Cdt1 actions might be negatively regulated by both geminin and Cdks. Alternatively interaction between Cdt1 and geminin could be under the control of Cdks. In certain cell types, Cdt1 is degraded on entry into the S phase (26), which could be directed by Cdk phosphorylation. However, the functional relationship between the Cdt1-geminin system and Cdks remains to be clarified.

In this report, we demonstrate that Cdt1 is phosphorylated by cyclin A-dependent kinases (cyclin A-Cdk1 and cyclin A-Cdk2) dependent on its cyclin-binding motif. Cdk phosphorylation resulted in Cdt1 binding to the F-box protein Skp2 (27), a component of the Skp1-Cdc53-F-box protein (SCF) ubiquitin ligase complex, and subsequent degradation. In contrast, *in vitro* DNA binding activity of Cdt1 was reduced by the phosphorylation. However, geminin binding to Cdt1 was not affected by the phosphorylation. Finally we show that Cdk1 inactivation results in Cdt1 dephosphorylation and rebinding to chromatin in murine FT210 cells. These findings suggest that Cdt1 function is negatively regulated by Cdk phosphorylation independent of geminin binding.

EXPERIMENTAL PROCEDURES

Construction of Expression Vectors for Human Cdt1 and Geminin and Murine Skp2—Cloning of human Cdt1 and geminin cDNAs and construction of mammalian expression vectors (based on pcDEBΔ or pcDEBΔ-T7) were described previously (26). To generate a mutant Cdt1 (Cdt1 Cy) in which Arg-68, Arg-69, and Leu-70 were all converted into Ala, site-directed mutagenesis was performed with oligonucleotide CAGGCCACCGGCCCGCGCTGCAGCGCGGCTGTCGGTGGACGAG using Mutan-Super Express Km kit (Takara), and the product of the resultant cDNA was confirmed by sequencing. For bacterial expression of glutathione *S*-transferase (GST)-Cdt1, the Cdt1 cDNA was introduced into pGEX-6P-1 (Amersham Biosciences), and for *in vitro* production of His-geminin with bacterial lysate, the geminin cDNA was inserted into pIVEX2.4b Nde (Roche Applied Science). Plasmid pcDNA3-HA-Skp2 (27), in which hemagglutinin (HA)-tagged murine Skp2 cDNA is transcribed from the T7 promoter, was kindly provided by Dr. K. Nakayama (Kyushu University).

Antibodies—Preparation of polyclonal rabbit antibodies against human Cdt1 and MCM7 was as described previously (26, 28). Other antibodies used were purchased from different companies: Cdt1 (N-20, Santa Cruz Biotechnology), T7 tag (Novagen), HA tag (BAbCO), GST (G7781, Sigma), geminin (C-16 and N-19, Santa Cruz Biotechnology), cyclin A (BF683, Pharmingen), cyclin B (GNS-1, Pharmingen), Cdk1 (C-4973, Sigma), Cdk2 (558896, Pharmingen), Skp2 (H-435, Santa Cruz Biotechnology), p27 (K25020, Transduction Laboratories), actin (MAB1501, Chemicon).

Preparation of Cyclin-Cdks Using Recombinant Baculoviruses—GST-murine cyclin A and GST-murine cyclin B baculoviruses were provided by Dr. H. Masai (Tokyo Metropolitan Institute of Medical Science), and human Cdk1 and Cdk2 baculoviruses were purchased from Orbigen (San Diego, CA). At 48 h after infection (multiplicity of infection of 2 for GST-cyclins and 5 for Cdks) of 2×10^8 High Five cells with recombinant baculoviruses, extracts were prepared with 5 ml of lysis buffer (50 mM Tris-HCl, pH 7.4, 100 mM NaCl, 0.1% Nonidet P-40, 10% glycerol, 1 mM dithiothreitol (DTT)) containing multiple protease inhibitors (Sigma). The lysates were clarified by centrifugation and filtration, and GST-cyclin-Cdk complexes were purified with 1.5 ml of glutathione-Sepharose beads (Amersham Biosciences). The beads were then resuspended in thrombin cleavage buffer (50 mM Tris-HCl, pH 7.4, 150 mM NaCl, 2.5 mM $CaCl_2$, 10% glycerol) and digested with 20 units of thrombin (Amersham Biosciences) for 45 min at room temperature to allow the cyclin-Cdks to be eluted. The purity of the cyclin-Cdk complexes was confirmed by SDS-PAGE followed by silver staining and immunoblotting. The approximate concentrations of the obtained cyclin-Cdks were estimated to be as follows: 1 ng/μl for cyclin A-Cdk1 and cyclin B-Cdk1 and 10 ng/μl for cyclin A-Cdk2.

Production of Recombinant GST-Cdt1, His-geminin, and HA-Skp2 Proteins—GST-Cdt1 and a GST-Cdt1 Cy mutant were produced in *Escherichia coli* strain BL-21, purified on glutathione-Sepharose beads, eluted with 20 mM glutathione in elution buffer A (200 mM NaCl, 20 mM Tris-HCl, pH 7.4, 1 mM DTT, 0.05% Triton X-100), and dialyzed. His-tagged Geminin proteins were synthesized using an *in vitro* transcription-translation system with bacterial extracts (RTS 500, Roche Applied Science) according to the manufacturer's instructions, purified on nickel affinity gel (Sigma), eluted with elution buffer B (50 mM sodium phosphate, pH 8.0, 250 mM NaCl) containing 250 mM imidazole, and dialyzed. HA-tagged Skp2 proteins were synthesized by *in vitro* transcription-translation with rabbit reticulocyte lysate (TnT T7 quick coupled transcription/translation system, Promega) according to the manufacturer's instructions.

In Vitro Kinase Assays—GST-Cdt1 (0.6 μg) or histone H1 (5 μg) were phosphorylated by the cyclin-Cdk complexes (approximately 5–10 ng) in 25 μl of kinase buffer (100 mM NaCl, 50 mM Tris-Cl, pH 7.5, 10 mM $MgCl_2$, 1 mM EGTA, 2.5 mM DTT, 0.025% Triton X-100, 5% glycerol, 80 μM ATP, 1 μM calyculin A, 1 mM phenylmethylsulfonyl fluoride, 10 mM glycerophosphate) containing 10μCi of [γ-^{33}P]ATP (Amersham Biosciences) at 30 °C for 30 min. The reactions were stopped by the addition of 4× sample buffer (1× sample buffer: 62.5 mM Tris-HCl, pH 6.8, 2% SDS, 5% β-mercaptoethanol, 10% glycerol, 0.01% bromphenol blue) and processed for SDS-PAGE. The gels were stained with Coomassie Blue, dried, and analyzed with bioimaging analyzer BAS 2500 (Fuji Film).

In Vitro Binding Assays—For assaying the association of Cdt1 with cyclin-Cdks, a 3-μg aliquot of GST-Cdt1 was incubated with 10–50 ng of cyclin-Cdks in binding buffer A (200 mM NaCl, 20 mM Tris-HCl, pH 7.4, 1 mM DTT, 0.05% Triton X-100, 5% glycerol) containing 1 μM calyculin A, 10 mM glycerophosphate, and 1 mM phenylmethylsulfonyl fluoride at 4 °C for 60 min. Then the GST fusion proteins were collected on glutathione beads, and the beads were washed three times with binding buffer A. The bound proteins were eluted with 25 μl of 1× sample buffer and analyzed by immunoblotting.

Cdt1-geminin interaction was assessed as follows. GST-Cdt1 (0.6 μg) and His-geminin (0.2 μg) were subjected to phosphorylation reaction as described above except that radiolabeled ATP was omitted. The mixtures were diluted with binding buffer A, and binding reactions were carried out at 4 °C for 60 min. Then the GST-Cdt1 and associated His-geminin proteins were analyzed as described above.

Cdt1-Skp2 interaction was assessed as follows. GST-Cdt1 (0.6 μg) was subjected to phosphorylation reactions as described above with or without the cyclin-Cdks, mixed with the HA-Skp2 produced by *in vitro* translation in 50 μl of reaction mixture, diluted with binding buffer B (100 mM NaCl, 20 mM Tris-HCl, pH 7.4, 0.1% Triton X-100) containing 10 mM glycerophosphate and 5 mM NaF, and incubated at 4 °C for 60 min. Then the GST-Cdt1 and associated Skp2 proteins were collected, washed with binding buffer A, and analyzed.

DNA binding activity of Cdt1 was examined as follows. GST-Cdt1 (0.6 μg) was subjected to reaction with or without the cyclin-Cdks as above, diluted with binding buffer B, and incubated with 30 μl of double-stranded DNA cellulose beads (Amersham Biosciences) at 4 °C for 90 min. Then the beads were washed three times with binding buffer A, and the associated proteins were analyzed by immunoblotting.

Transfection, Immunoprecipitation, and Immunoblotting—293T cells were grown in Dulbecco's modified Eagle's medium with 8% fetal calf serum. The indicated plasmids (6 μg) were transiently transfected into 4×10^6 cells in 100-mm dishes with TransIT-293 reagent (Mirus, Madison, WI) according to the manufacturer's instructions. When indicated, cell were synchronized in G_2/M phase with 50 ng/ml nocodazole treatment for 14–18 h.

After 48 h, cells were lysed on ice in 1 ml of Nonidet P-40 buffer (150 mM NaCl, 1% Nonidet P-40, 10 mM Tris-HCl, pH 7.4) containing multiple protease inhibitors, and the soluble fraction was separated by centrifugation. Aliquots of the lysates were immunoprecipitated with anti-T7 antibody- or control IgG-fixed beads (Novagen), and the beads were washed four times with 1 ml of NET gel buffer (50 mM Tris-HCl, pH 7.4, 150 mM NaCl, 0.1% Triton X-100, 1 mM EDTA). The immunoprecipitates were eluted with the elution buffer (100 mM glycine-HCl, pH 2.5) and subjected to immunoblotting.

Immunoblotting was performed as described previously (20). Antibody binding was visualized using the ECL system (Amersham Biosciences).

Establishment of Rat-1 Cells Stably Expressing T7-tagged Cdt1—Rat-1 cells (normal rat fibroblasts) were grown in Dulbecco's modified Eagle's medium with 8% fetal calf serum. Recombinant retroviruses expressing wild type T7-tagged human Cdt1 or T7-Cdt1 Cy were prepared, and cells were infected with the viruses. Cells were then selected with hygromycin B and cloned. Representative lines expressing wild type T7-Cdt1 (designated WB4) or T7-Cdt1 Cy (designated CB3) were established and used for further study. The levels of T7-Cdt1 in these

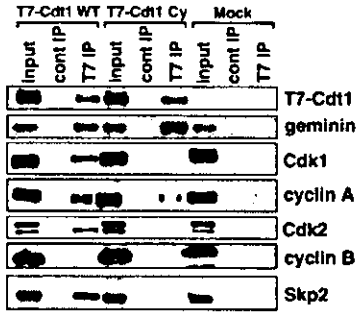

FIG. 1. ***In vivo* interaction of Cdt1 with various cell cycle-regulating proteins and the role of the Cy motif.** After transfection into 293T cells, T7-tagged wild type Cdt1 or the cyclin-binding motif-mutated Cdt1 (Cdt1 Cy) were immunoprecipitated with anti-T7 antibody beads, and immunoprecipitates were subjected to immunoblotting with the indicated antibodies to detect Cdt1-associated proteins. Ten percent of the input sample (*input*) was analyzed with the precipitate (*IP*) to show the precipitation efficiency. *cont*, control antibody.

cells were about 20 times those of endogenous Cdt1. Details of establishment and characterization of these cells will be published elsewhere.[2] When indicated, cells were synchronized in S phase with 2.5 mM hydroxyurea treatment for 18 h.

λ-Phosphatase Treatment of Cdt1-Geminin Complexes Immunoprecipitated from 293T Cells—Cdt1-geminin complexes were immunoprecipitated with anti-T7 antibody from 293T cells transfected with Cdt1 and T7-geminin and synchronized in G_2/M phase with nocodazole. After washing, the purified immunoprecipitates were treated with 100 units of λ-phosphatase (New England Biolabs) in 50 μl of phosphatase buffer (50 mM Tris-HCl, pH 7.8, 5 mM DTT, 2 mM $MnCl_2$, 1 mM phenylmethylsulfonyl fluoride) for 30 min at 30 °C or left untreated in the same buffer. Then proteins released into supernatants or remaining on the beads were separated by centrifugation and subjected to immunoblotting.

Cdk1 Inactivation in Temperature-sensitive Murine FT210 Cells—FT210 cells (17, 19, 29) were maintained at 32 °C in RPMI 1640 medium containing 25 mM Hepes and 10% fetal calf serum. For G_2/M synchronization, cells were treated with 50 ng/ml nocodazole for 16 h at either 32 °C or 39 °C. Cell fractionation was performed as described previously (17, 19).

RESULTS

Cyclin A-dependent Kinases, but Not Cyclin B-Cdk1, Bind to Human Cdt1 through the Cyclin-binding Motif—To explore functional associations between Cdt1 and Cdks, we first assessed physical interactions *in vivo* by immunoprecipitation with anti-T7 tag antibody after transfection of T7-tagged Cdt1 into 293T cells (Fig. 1). Cyclin A, Cdk1, and Cdk2, but not cyclin B, proteins were specifically co-precipitated with T7-Cdt1. Cdt1 has a putative cyclin-binding motif (7, 8, 30, 31) in the N terminus. To test its role, we created a T7-Cdt1 mutant in which the conserved Arg-68, Arg-69, and Leu-70 (Cy motif) had been substituted with alanines (T7-Cdt1 Cy). When T7-Cdt1 Cy was introduced into 293T cells and analyzed by immunoprecipitation as above, no or reduced co-precipitation of cyclin A, Cdk1, and Cdk2 was evident (Fig. 1). These data suggest that Cdt1 may interact with cyclin A-Cdk1 and cyclin A-Cdk2 kinases through the Cy motif. We sought to co-precipitate cyclin A-Cdks with endogenous Cdt1 but failed to do so (data not shown). Therefore, physical interaction between Cdt1 and cyclin A-Cdks may not be very strong. However, as described below, further studies clearly demonstrate that this interaction plays a crucial role in phosphorylation and regulation of Cdt1 by cyclin A-dependent kinases.

We next set up an *in vitro* assay system. Bacterially produced purified wild type GST-Cdt1 and GST-Cdt1 Cy fusion proteins were incubated with cyclin A-Cdk1, cyclin A-Cdk2, and cyclin B-Cdk1 complexes generated in the baculoviral system and purified. Then the GST fusion proteins were collected on glutathione beads, and associated cyclin-Cdks were analyzed by immunoblotting. As shown in Fig. 2*A*, cyclin A-Cdk1 and cyclin A-Cdk2, but not cyclin B-Cdk1, efficiently bound to GST-Cdt1, whereas no specific binding was noted to GST-Cdt1 Cy or to GST alone (data not shown) under the same conditions. Lower bands observed both in cyclin A and cyclin B samples may be truncated forms nonspecifically cleaved by thrombin, but the kinase complexes have sufficient activities as mentioned below. Taken together, these data clearly demonstrate that cyclin A-Cdk1 and cyclin A-Cdk2 kinases directly bind to Cdt1 through the Cy motif.

Cyclin A-dependent Kinases Phosphorylate Cdt1 Depending on Their Binding to the Cyclin-binding Motif—The obtained data suggested that Cdt1 could be a good substrate for cyclin A-dependent kinases. Therefore, we performed an *in vitro* phosphorylation assay with [γ-^{33}P]ATP. When histone H1 proteins were used as the substrate, all three cyclin-Cdks demonstrated similar phosphorylation under our assay conditions (Fig. 2*B*). However, the A- and B-type cyclin-Cdk complexes varied significantly in their ability to phosphorylate Cdt1. Both cyclin A-Cdk1 and cyclin A-Cdk2 were about 6–8-fold more active toward GST-Cdt1 than the cyclin B-Cdk1 (Fig. 2*B*). Furthermore GST-Cdt1 phosphorylation by the cyclin A-dependent kinases specifically retarded its electrophoretic mobility. As expected, this efficient phosphorylation required binding of the cyclin A-dependent kinases to Cdt1 via the Cy motif (Fig. 2, *A* and *B*). It was also notable that phosphorylation efficacy of Cdt1 by the two cyclin A-dependent kinases was virtually the same and that similar electrophoretic retardation was observed after the phosphorylation, suggesting that their phosphorylation sites in Cdt1 may be very similar *in vitro*.

We then asked whether Cdt1 is phosphorylated by cyclin A-dependent kinases *in vivo* as well as *in vitro*. However, a problem to be overcome in this context is that Cdt1 itself is degraded during the S, G_2, and M phases (26) when cyclin A-dependent kinases are active. Especially given that Cdt1 phosphorylated by cyclin A-dependent kinases is targeted for degradation (see below), we anticipated that it would be difficult to analyze this *in vivo*. One possibility for dealing with phosphorylated Cdt1 may be to treat cells with proteasome inhibitors. Previously it was shown that phosphorylated and thus more slowly migrating Cdt1 becomes detectable following proteasome inhibitor treatment (26, 32). Another possibility may be to synchronize cells in the G_2/M phase through activation of a spindle checkpoint pathway with nocodazole treatment (26), although the mechanism is unknown. Indeed we also detected a slow migrating form of Cdt1 in 293T cells synchronized in the G_2/M phase with nocodazole that disappeared with λ-phosphatase treatment (Fig. 3*B*; for details, see below). If such phosphorylation were carried out by cyclin A-dependent kinases, it would be expected to be lacking with Cdt1 Cy. To test this, 293T cells were transfected with either wild type T7-Cdt1 or T7-Cdt1 Cy and synchronized around G_2/M phase with nocodazole treatment. Then whole cell lysates were prepared and analyzed by immunoblotting with anti-T7 antibody. As expected, the hyperphosphorylated and slow migrating form of Cdt1 was observed with the wild type but was undetectable with Cdt1 Cy (Fig. 2C). Taken together, these data lead us to conclude that Cdt1 is phosphorylated by cyclin A-Cdks *in vivo*.

Cdt1 Phosphorylation by Cyclin A-dependent Kinases Does Not Affect the Binding to Geminin—It has been suggested that inhibition of Cdt1 function by geminin is not associated with

[2] Y. Tatsumi, N. Sugimoto, T. Kiyono, and M. Fujita, manuscript in preparation.

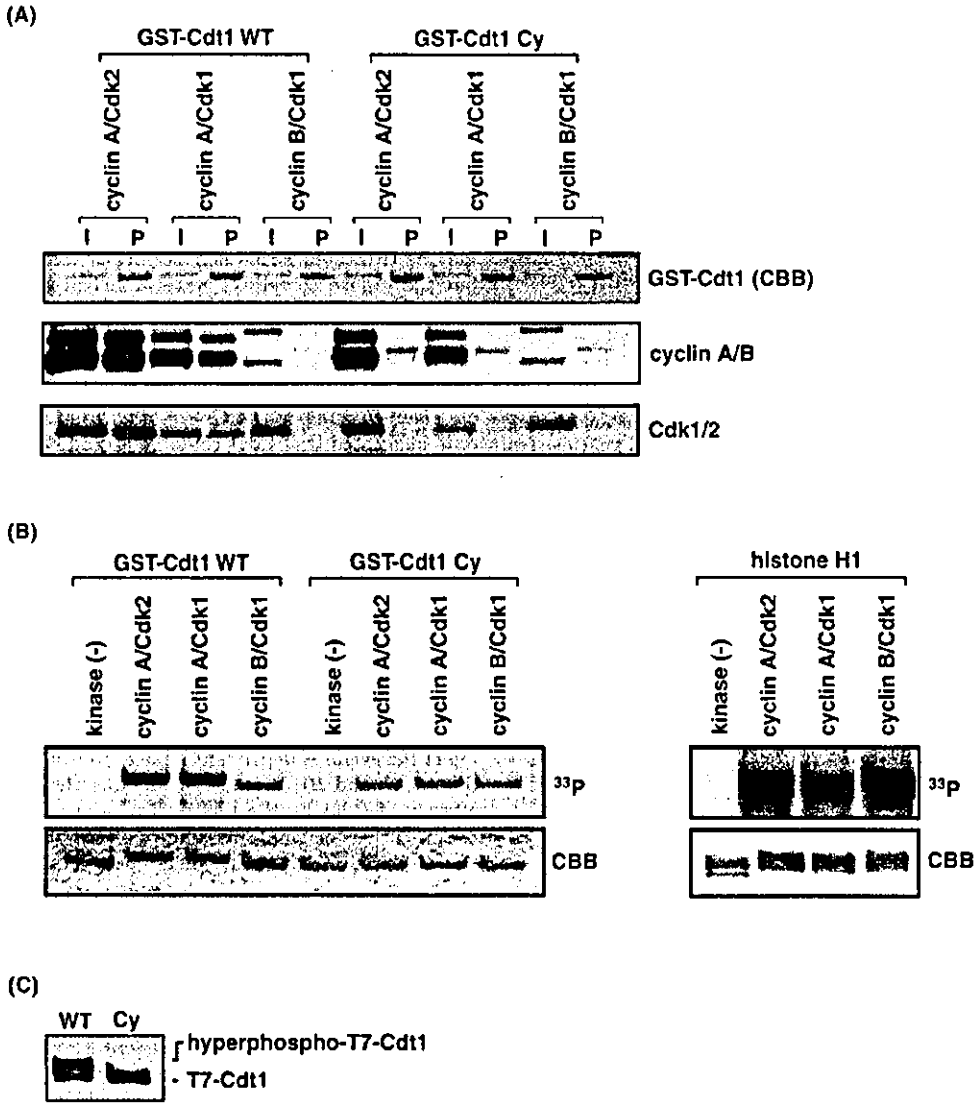

FIG. 2. **Cyclin A-Cdk complexes specifically bind to and phosphorylate human Cdt1 depending on the cyclin-binding motif.** *A*, bacterially produced GST-Cdt1 was incubated with cyclin A-Cdk1, cyclin A-Cdk2, or cyclin B-Cdk1 purified from baculovirus-infected cells. Then GST fusion and associated proteins were collected on glutathione beads and subjected to Coomassie Blue staining (*top panel*) or to immunoblotting with mixtures of the anti-cyclin A and anti-cyclin B antibodies (*middle panel*) or the anti-Cdk1 and anti-Cdk2 antibodies (*lower panel*). Ten percent of the input sample (*I*) was analyzed with the precipitate (*P*). *B*, GST-Cdt1 or histone H1 were phosphorylated by the cyclin-Cdk complexes in the presence of 10μCi of [γ-^{33}P]ATP and processed for SDS-PAGE. The gels were stained with Coomassie Blue, dried, and analyzed with bioimaging analyzer BAS 2500 to measure incorporated radioactivity. *C*, 293T cells were transfected with either wild type T7-Cdt1 or T7-Cdt1 Cy and synchronized around G_2/M phase with nocodazole treatment. Then the whole cell lysates were prepared and analyzed by immunoblotting with anti-T7 antibody. *CBB*, Coomassie Brilliant Blue; *WT*, wild type.

Cdk activity (25). On the other hand, ablation of Cdk1 kinase leads to rebinding of MCM and subsequent rereplication (16, 17), leaving a possible regulatory role for Cdks in the Cdt1-geminin interaction. To this end, we examined whether Cdk phosphorylation alters the affinity of Cdt1 for geminin *in vitro*. GST-Cdt1 and His-geminin produced by bacterial extracts and purified were mixed and subjected to kinase reactions with the three cyclin-Cdks. Under our experimental conditions, geminin was also phosphorylated by the Cdks although inefficiently (data not shown). The mixtures were then diluted with buffer and subjected to precipitation with glutathione beads. Remarkable amounts of His-geminin were bound to GST-Cdt1, and the efficacy was not changed by Cdt1 phosphorylation by the cyclin A-dependent kinases as confirmed by mobility shifts (Fig. 3*A*). No His-geminin was co-precipitated with GST alone (Fig. 3*A*). Therefore, it is unlikely that Cdt1 phosphorylation by Cdks affects the binding to geminin.

The notion was further supported by different approaches as follows. 293T cells were transfected with expression vectors encoding Cdt1 and T7-geminin and synchronized at G_2/M with nocodazole. Cell lysates were then prepared, immunoprecipitated with anti-T7 antibodies, and analyzed by immunoblotting with anti-Cdt1 and anti-T7 antibodies. In G_2/M phase 293T cells, the slow migrating form of Cdt1 was found in addition to the normally migrating form, and both were similarly co-precipitated with T7-geminin (Fig. 3*B*). On treatment of the immunoprecipitates with λ-phosphatase, the slow migrating form disappeared (Fig. 3*B*), consistent with it being Cdt1 phosphorylated by cyclin A-dependent kinases. The treatment resulted in no detachment of Cdt1 from T7-geminin (Fig. 3*B*). Another

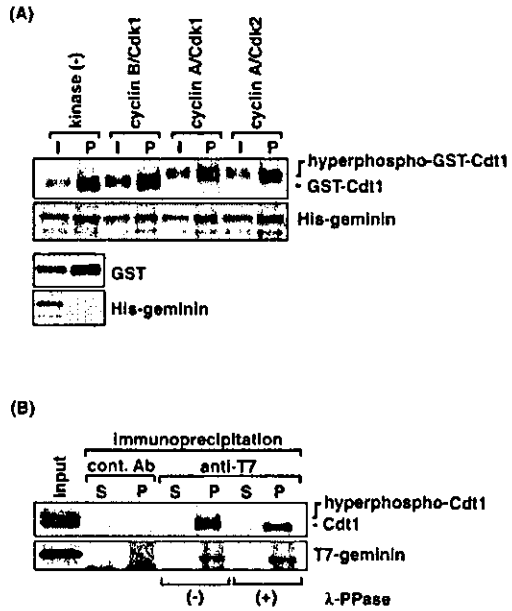

FIG. 3. **Cdt1 phosphorylation by cyclin A-Cdk complexes does not affect its binding affinity for geminin.** *A*, *in vitro* assay for Cdt1-geminin binding. GST-Cdt1 and His-geminin synthesized by *in vitro* translation with bacterial lysates were subjected to phosphorylation reactions without radiolabeled ATP. Then GST fusion and associated proteins were collected on glutathione beads and subjected to immunoblotting with anti-Cdt1 or anti-geminin antibodies. As a negative control, GST and His-geminin were subjected to the same assay without a phosphorylation reaction. Ten percent of the input sample (*I*) was analyzed with the precipitate (*P*). *B*, phosphatase treatment of immunopurified Cdt1-geminin complexes. Cdt1-geminin complexes were immunoprecipitated with anti-T7 antibody from 293T cells transfected with Cdt1 and T7-tagged geminin and synchronized in G_2/M phase with nocodazole. The purified immunoprecipitates were treated with λ-phosphatase or left untreated. Then proteins released into supernatants (*S*) or remaining on the beads (*P*) were separated by centrifugation and subjected to immunoblotting with anti-T7 or anti-Cdt1 antibodies. *cont.*, control; *Ab*, antibody; *PPase*, phosphatase.

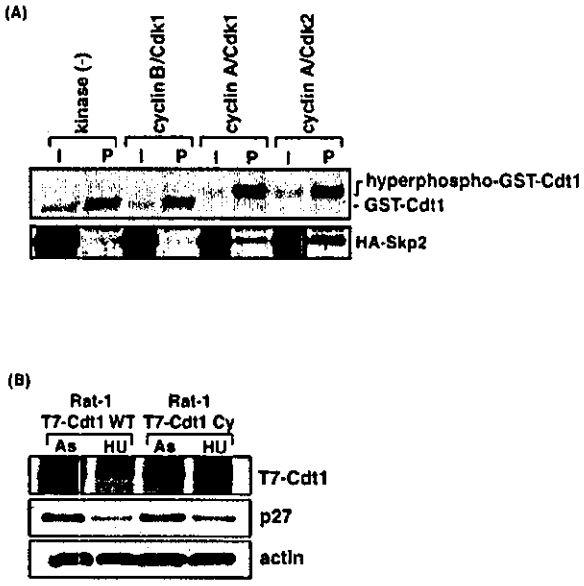

FIG. 4. **Association of Cdt1 with Skp2 is dependent on phosphorylation by cyclin A-dependent kinases and results in its degradation.** *A*, *in vitro* binding of Skp2 to Cdt1 phosphorylated by cyclin A-dependent kinases. GST-Cdt1 was subjected to reaction with or without the cyclin-Cdks and mixed with HA-tagged Skp2 proteins synthesized by *in vitro* transcription-translation with rabbit reticulocyte lysate. Then the GST-Cdt1 and associated Skp2 proteins were collected on glutathione beads and analyzed by immunoblotting with anti-Cdt1 or anti-HA antibodies. Ten percent of the input sample (*I*) was analyzed with the precipitate (*P*). *B*, phosphorylation-deficient Cdt1 Cy mutant is partially resistant to S phase degradation. Rat-1 cells stably expressing wild type T7-Cdt1 or its Cy mutant were established. Whole cell lysates were prepared from the cells either synchronized in S phase by hydroxyurea treatment or left asynchronous and subjected to immunoblotting with anti-T7, anti-p27, or anti-actin antibodies. *As*, asynchronous; *HU*, hydroxyurea.

approach taken was to investigate whether T7-Cdt1 Cy, which cannot be phosphorylated by cyclin A-dependent kinases as above, could bind to geminin *in vivo*. As shown in Fig. 1, no apparent difference in association with geminin was observed between wild type Cdt1 and Cdt1 Cy. Together these data clearly show that the interaction between Cdt1 and geminin is not affected by Cdk phosphorylation.

Association of Cdt1 with the F-box Protein Skp2 Requires Phosphorylation by Cyclin A-dependent Kinases and Leads to Cdt1 Degradation—At least in certain cell types, the levels of Cdt1 proteins are decreased as they enter S phase (26). This appears to be due to the ubiquitin-proteasome system (26). Very recently it has been shown that Cdt1 binds to Skp2 depending on its phosphorylation, although the kinase responsible has not yet been identified (32). Independently we also found Skp2 to be co-precipitated with T7-Cdt1 (Fig. 1; for details, see below). Skp2 is an F-box protein mediating the ubiquitination of target proteins by the SCF ubiquitin ligase complex (27). Therefore, it is presumable that ubiquitination of Cdt1 by the SCF^{Skp2} complex may lead to its degradation after S phase (32). We considered that Cdt1 phosphorylation required for Skp2 binding might be achieved by cyclin A-dependent kinases and investigated this possibility by *in vitro* binding assay. Recombinant Skp2 proteins were obtained by *in vitro* translation with rabbit reticulocyte lysate and subjected to binding assays with GST-Cdt1 treated with or without cyclin-Cdks. When GST-Cdt1 proteins were unphosphorylated or phosphorylated with cyclin B-Cdk1, no binding to Skp2 was observed (Fig. 4*A*). In clear contrast, significant binding was detected when GST-Cdt1 was hyperphosphorylated with cyclin A-dependent kinases (Fig. 4*A*). The reason for the relatively inefficient association observed is unclear at present, but considering that *in vivo* interaction between them detected by immunoprecipitation appears more efficient (see below), other components of SCF complex such as Skp1 would be required for the efficient recognition of Cdt1 by Skp2. Another problem is that cyclin A-Cdk2 phosphorylation of GST-Cdt1 appears to enhance binding to Skp2 more efficiently than cyclin A-Cdk1 phosphorylation. This finding proved repeatable in multiple experiments and thus suggests the possibility that there are differences in some phosphorylation site(s) in Cdt1 when phosphorylated by the two kinases, affecting its affinity for Skp2. If this were the case, it would be of interest and should be addressed in the future.

The data obtained with the *in vitro* assays indicate that Cdt1 phosphorylation by cyclin A-dependent kinases, which is dependent on the Cy motif, is required for the Skp2 binding. It was therefore predicted that wild type Cdt1, but not Cdt1 Cy, interacts with Skp2 *in vivo*. As shown in Fig. 1, wild type T7-Cdt1 efficiently co-immunoprecipitated Skp2 from 293T cell extracts, while T7-Cdt1 Cy could not, indicating that Cdt1 phosphorylation by cyclin A-dependent kinases also plays a crucial role in the Skp2 binding *in vivo*.

If recognition of the phosphorylated Cdt1 by Skp2 in fact results in its degradation after S phase, then the Cdt1 Cy mutant would be resistant to this. To test this prediction, we established Rat-1 cells stably expressing wild type T7-Cdt1 or

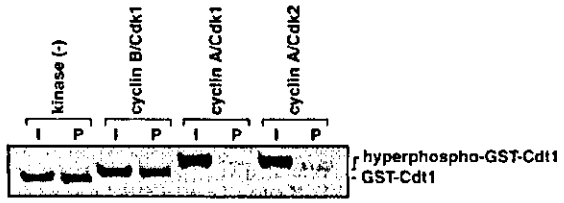

FIG. 5. **Cdt1 phosphorylation by cyclin A-Cdk complexes diminishes its affinity for double-stranded DNA *in vitro*.** GST-Cdt1 was subjected to phosphorylation and loaded onto double-stranded DNA cellulose beads. Then the beads were washed three times, and the bound proteins were analyzed by immunoblotting with anti-Cdt1 antibodies. Forty percent of the input sample (*I*) was analyzed with the precipitate (*P*).

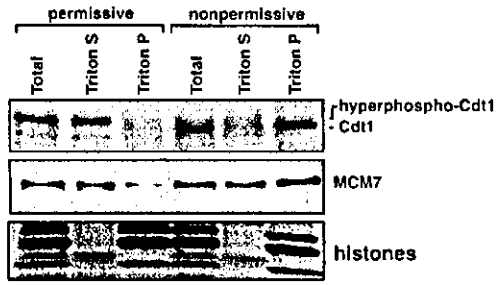

FIG. 6. **Cdk1 inactivation in murine Cdk1 kinase temperature-sensitive mutant FT210 cells results in Cdt1 dephosphorylation and rebinding to chromatin/nuclear matrix.** FT210 cells were incubated with nocodazole for 16 h at permissive (32 °C) or non-permissive (39 °C) temperatures. Whole cell extracts (*Total*), Triton X-100-extractable fractions (*Triton S*), and nuclear chromatin/matrix fractions (*Triton P*) were prepared from the cells and immunoblotted with anti-Cdt1 or anti-MCM7 antibodies. The samples were also subjected to SDS-PAGE followed by Coomassie Blue staining for detection of core histones.

its Cy mutant as described under "Experimental Procedures." Whole cell lysates were prepared from cells either synchronized in S phase with hydroxyurea or left asynchronous and then immunoblotted with anti-T7 antibody. The samples were also immunoblotted with anti-actin antibody for normalization. The levels of wild type T7-Cdt1 protein in the S phase cells were reduced to ~5% of those in the asynchronous cells (Fig. 4*B*). In contrast, the levels of T7-Cdt1 Cy protein in the S phase cells were reduced only to ~25% of those in the asynchronous cells (Fig. 4*B*). We also examined p27, a Cdk inhibitor, as an example of another protein that is degraded in an Skp2-dependent manner in S phase (27). In both cell lines, p27 protein levels were similarly reduced by about 50% by hydroxyurea treatment (Fig. 4*B*). These data indicate that Skp2 binding to Cdt1 phosphorylated by cyclin A-dependent kinases causes Cdt1 degradation in S phase. However, the data also demonstrate that there are other pathways involved in Cdt1 degradation.

Cdt1 DNA Binding Activity Is Reduced by Phosphorylation—Murine Cdt1 binds to DNA in a sequence-, strand- and conformation-independent manner (33). Given that this is an important property for Cdt1 function as an MCM loader, it would be expected that Cdt1 DNA binding activity is regulated by Cdk phosphorylation as well as by geminin binding (33). We therefore investigated whether human Cdt1 also has DNA binding activity and, if so, whether it is affected by Cdk phosphorylation. To this end, bacterially produced GST-Cdt1 was subjected to phosphorylation with the cyclin-Cdks as above, and using double-stranded DNA cellulose beads, the DNA binding activity was compared with the untreated case. While no specific binding of GST alone to DNA cellulose was observed (data not shown), the GST-Cdt1 demonstrated significant DNA binding, which was unaltered by phosphorylation with cyclin B-Cdk1 (Fig. 5). In contrast, GST-Cdt1 phosphorylated by cyclin A-dependent kinases had remarkably reduced affinity for DNA (Fig. 5).

Inhibition of Cdk1 Activity Results in Cdt1 Dephosphorylation and Rebinding to Chromatin in Murine FT210 Cells—We finally examined the *in vivo* role of Cdk1 in Cdt1 phosphorylation using murine Cdk1 kinase temperature-sensitive mutant FT210 cells (17, 19, 29). The cells were incubated with nocodazole for 16 h at permissive or non-permissive temperatures for synchronization at the G_2/M phase, and whole cell lysates, Triton X-100-extractable fractions, and nuclear pellets containing chromatin and non-chromatin nuclear structures were prepared. Immunoblotting with monoclonal antibody 4A4 specific for Cdk1-phosphorylated vimentin confirmed the Cdk1 inactivation at the non-permissive temperature (data not shown) as described previously (17). The samples were then immunoblotted with anti-Cdt1 antibodies, showing the presence of slow migrating hyperphosphorylated murine Cdt1 in the soluble fraction from the G_2/M phase FT210 cells cultured at the permissive temperature. In contrast, in cells cultured at the non-permissive temperature, Cdt1 was converted to the normally migrating form and became detectable mainly in the nuclear pellet fraction (Fig. 6), demonstrating Cdt1 dephosphorylation and rebinding to chromatin/nuclear matrix in the absence of Cdk1 activity. Consistent with the data we previously reported (17), reassociation of MCM7 with chromatin was also observed in cells lacking Cdk1 activity (Fig. 6). These data indicate that Cdt1 phosphorylation by Cdk1 kinase plays a crucial role in suppression of its functions *in vivo*.

DISCUSSION

Cyclin A-dependent Kinases Phosphorylate Cdt1 through Their Binding to the Cyclin-binding Motif—Our data demonstrate that cyclin A-dependent kinases efficiently phosphorylate Cdt1. This phosphorylation needs stable association of the cyclin-kinase complexes through the Cy motif of Cdt1. CDC6, which is ORC-dependently recruited onto chromatin and is required for MCM loading like Cdt1, is also phosphorylated by cyclin A-dependent kinases (6–8) and similarly harbors a conserved cyclin-binding motif, which is in fact required for cyclin-Cdk complex binding (8). However, the cyclin A-dependent kinases need not stably interact with CDC6 via the Cy motif to efficiently phosphorylate the protein (8), indicating that another site in CDC6 may mediate the specific but relatively unstable interaction with the cyclin A-Cdk. This is in contrast to what we have observed here for Cdt1. Since the Cy-mutated Cdt1 we made is actually refractory to Cdk phosphorylation, it will be useful to explore how the phosphorylation influences the Cdt1 function *in vivo*.

It was found that both cyclin A-Cdk1 and cyclin A-Cdk2 are similarly active toward Cdt1 phosphorylation, indicating that cyclin A targets the kinase complexes. In the mammalian somatic cell cycle, cyclin A-Cdk2 is believed to be the S phase-promoting Cdk (34–36), while cyclin B-Cdk1 is the mitotic Cdk (37). In addition, cyclin A-Cdk1 is active during S and G_2 phases (34). However, its biological functions remain to be fully addressed. Ablation of Cdk1 kinase activity results in rebinding of MCM proteins and subsequent rereplication (16, 17). On the other hand, ablation of cyclin A, but not cyclin B, leads to rereplication in *Drosophila* tissue culture cells (18). Taken together, the data suggest a crucial role of cyclin A-Cdk1 in prevention of rereplication. Indeed cyclin A-Cdk1 can phosphorylate Cdt1 as efficiently as cyclin A-Cdk2, leading to suppression of some Cdt1 functions as shown here. It has been reported that in mammalian cells CDC6 is phosphorylated by cyclin A-Cdk2, resulting in its nuclear export and canceling its functions (6, 7). Cyclin A-Cdk1 could execute the same function, although this has yet to be investigated. Very recently it was

shown that Cdk2 is dispensable for somatic cell cycling (38), while cyclin A is essential (36). Therefore, the cyclin A-Cdk1 could play important roles in both positive and negative regulation of replication. On the other hand, although our data demonstrate that cyclin A-dependent kinases play a crucial role in phosphorylation and regulation of Cdt1, we cannot exclude the possibility that cyclin B-Cdk1 might also function *in vivo*.

Cdt1 Phosphorylation by Cyclin A-dependent Kinases Does Not Affect the Binding to Geminin—In the absence of Cdk1 kinase activity, geminin is insufficient to completely suppress rereplication (17, 18), suggesting the possibility that geminin binding to Cdt1 is regulated by Cdk phosphorylation. However, our present data clearly indicate that this is not the case. Such aspect of regulation of geminin binding to Cdt1 might be favorable under certain conditions during the cell cycle; even when Cdk activity is down-regulated by the checkpoint mechanism in cells undergoing DNA damage, reformation of pre-RC could be prevented (1). However, during normal cell cycling, both Cdk phosphorylation and geminin may play indispensable roles in prohibition of rereplication.

Inhibitory Effects of Cdt1 Phosphorylation by Cyclin A-dependent Kinases—Cdk activity has a bipartite function in the cell cycle regulation of eukaryotic DNA replication, promoting replication and preventing rereplication (1, 2). Candidate molecules that should be phosphorylated by the Cdks to stimulate replication may include MCM and Sld2 proteins (1, 2, 39). It has been reported that the Cdks physically interact with and phosphorylate ORC and CDC6 (5–10). However, considering that they are no longer required for initiation reaction after loading MCM in an *in vitro* DNA replication system with *Xenopus* egg extracts (11, 12), such phosphorylation is likely to be involved in negative regulation. Indeed, in mammalian somatic cells, ORC1 protein is degraded after S phase (10, 20), and CDC6 is, at least partly, excluded from the nuclei through phosphorylation by Cdks (5–7, 19). It has also been shown that unphosphorylatable mutant CDC6 can support DNA replication in egg extracts (40).

The current concept is that Cdt1, together with ORC and CDC6 proteins, forms the machinery that loads MCM heterohexameric complexes onto prereplication chromosomal DNA (1, 2). By analogy with ORC and CDC6, Cdt1 might also be dispensable after loading MCM. Indeed it has been found that Cdt1 protein levels fall after S phase in certain cell types (26, 32). Therefore, it is very conceivable that Cdt1 phosphorylation by cyclin A-dependent kinases negatively regulates its function after S phase. Our data presented here support this notion. First, Cdt1 phosphorylated by cyclin A-dependent kinases is targeted for binding to Skp2 and subsequently degraded. It should also be noted, however, that other pathways exist that are involved in Cdt1 degradation after S phase (41). Prevention of Cdt1 function may be carried out not only by regulation at the protein level but also through effects on activity. In nocodazole-treated and spindle checkpoint-activated cells, levels of Cdt1 protein recover by unknown mechanisms (26), but they remain detached from chromatin as shown here. Also in a DNA replication system with egg extracts, Cdt1 is dissociated from chromatin after S phase without degradation (22). Since Cdk1 inactivation leads to Cdt1 dephosphorylation and rebinding accompanied by MCM reassociation, inhibition of the Cdt1 chromatin rebinding may depend on the Cdk1 phosphorylation. Our finding that Cdt1 phosphorylation by cyclin A-dependent kinases reduces its affinity to DNA provides one possible explanation for such inhibition. Overall the data lead us to conclude that Cdt1 phosphorylation by cyclin A-dependent kinases plays crucial roles in negative regulation of its function after S phase. Indeed we have observed that the ability of the Cy-mutated Cdt1 to induce activation of the ATM (ataxia telangiectasia-mutated) checkpoint pathway and subsequent rereplication in the overexpressed cell is higher than the wild type despite similar binding affinity for geminin.[2]

Acknowledgments—We thank M. Itoh and Y. Nishikawa for technical assistance and M. Noda and Y. Hanada for secretarial work. We are also grateful to Drs. K. Nakayama and H. Masai for providing the Skp2 expression vectors and cyclin baculoviruses, respectively.

REFERENCES

1. Bell, S. P., and Dutta, A. (2002) *Annu. Rev. Biochem.* **71,** 333–374
2. Fujita, M. (1999) *Front. Biosci.* **4,** D816–D823
3. Ishimi, Y. (1997) *J. Biol. Chem.* **272,** 24508–24513
4. Labib, K., Tercero, J. A., and Diffley, J. F. (2000) *Science* **288,** 1643–1647
5. Saha, P., Chen, J., Thome, K. C., Lawlis, S. J., Hou, Z. Hendricks, M., Parvin, J. D., and Dutta, A. (1998) *Mol. Cell. Biol.* **18,** 2758–2767
6. Jiang, W., Wells, N. J., and Hunter, T. (1999) *Proc. Natl. Acad. Sci. U. S. A.* **96,** 6193–6198
7. Petersen, B. O., Lukas, J., Sørensen, C. S., Bartek, J., and Helin, K. (1999) *EMBO J.* **18,** 396–410
8. Herbig, U., Griffith, J. W., and Fanning, E. (2000) *Mol. Biol. Cell* **11,** 4117–4130
9. Nguyen, V. Q., Co, C., and Li, J. J. (2001) *Nature* **411,** 1068–1073
10. Méndez, J., Zou-Yang, X. H., Kim, S., Hidaka, M., Tansey, W. P., and Stillman, B. (2002) *Mol. Cell* **9,** 481–491
11. Rowles, A., Tada, S., and Blow, J. J. (1999) *J. Cell Sci.* **112,** 2011–2018
12. Hua, X. H., and Newport, J. (1998) *J. Cell Biol.* **140,** 271–281
13. Zou, L., and Stillman, B. (1998) *Science* **280,** 593–596
14. Mimura, S., and Takisawa, H. (1998) *EMBO* **17,** 5699–5707
15. Arata, Y., Fujita, M., Ohtani, K., Kijima, S., and Kato, J. (2000) *J. Biol. Chem.* **275,** 6337–6345
16. Itzhaki, J. E., Gilbert, C. S., and Porter, A. C. (1997) *Nat. Genet.* **15,** 258–265
17. Fujita, M., Yamada, C., Tsurumi, T., Hanaoka, F., Matsuzawa, K., and Inagaki, M. (1998) *J. Biol. Chem.* **273,** 17095–17101
18. Mihaylov, I. S., Kondo, T., Jones, L., Ryzhikov, S., Tanaka, J., Zheng, J., Higa, L. A., Minamino, N., Cooley, L., and Zhang, H. (2002) *Mol. Cell. Biol.* **22,** 1868–1880
19. Fujita, M., Yamada, C., Goto, H., Yokoyama, N., Kuzushima, K., Inagaki, M., and Tsurumi, T. (1999) *J. Biol. Chem.* **274,** 25927–25932
20. Fujita, M., Ishimi, Y., Nakamura, H., Kiyono, T., and Tsurumi, T. (2002) *J. Biol. Chem.* **277,** 10354–10361
21. McGarry, T. J., and Kirschner, M. W. (1998) *Cell* **93,** 1043–1053
22. Maiorano, D., Moreau, J., and Méchali, M. (2000) *Nature* **404,** 622–625
23. Nishitani, H., Lygerou, Z., Nishimoto, T., and Nurse, P. (2000) *Nature* **404,** 625–628
24. Wohlschlegel, J. A., Dwyer, B. T., Dhar, S. K., Cvetic, C., Walter, J. C., and Dutta, A. (2000) *Science* **290,** 2309–2312
25. Tada, S., Li, A., Maiorano, D., Méchali, M., and Blow, J. J. (2001) *Nat. Cell Biol.* **3,** 107–113
26. Nishitani, H., Taraviras, S., Lygerou, Z., and Nishimoto, T. (2001) *J. Biol. Chem.* **276,** 44905–44911
27. Nakayama, K., Nagahama, H., Minamishima, Y. A., Matsumoto, M., Nakamichi, I., Kitagawa, K., Shirane, M., Tsunematsu, R., Tsukiyama, T., Ishida, N., Kitagawa, M., Nakayama, K., and Hatakeyama, S. (2000) *EMBO J.* **19,** 2069–2081
28. Fujita, M., Kiyono, T., Hayashi, Y., and Ishibashi, M. (1996) *J. Biol. Chem.* **271,** 4349–4354
29. Hamaguchi, J. R., Tobey, R. A., Pines, J., Crissman, H. A., Hunter, T., and Bradbury, E. M. (1992) *J. Cell Biol.* **117,** 1041–1053
30. Adams, P. D., Sellers, W. R., Sharma, S. K., Wu, A. D., Nalin, C. M., and Kaelin, W. G. (1996) *Mol. Cell. Biol.* **16,** 6623–6633
31. Chen, J., Saha, P., Kornbluth, S., Dynlacht, B. D., and Dutta, A. (1996) *Mol. Cell. Biol.* **16,** 4673–4682
32. Li, X., Zhao, Q., Liao, R., Sun, P., and Wu, X. (2003) *J. Biol. Chem.* **278,** 30854–30858
33. Yanagi, K., Mizuno, T., You, Z., and Hanaoka, F. (2002) *J. Biol. Chem.* **277,** 40871–40880
34. Pagano, M., Pepperkok, R., Verde, F., Ansorge, W., and Draetta, G. (1992) *EMBO J.* **11,** 961–971
35. Rosenblatt, J., Gu, Y., and Morgan, D. O. (1992) *Proc. Natl. Acad. Sci. U. S. A.* **89,** 2824–2828
36. Murphy, M., Stinnakre, M. G., Senamaud-Beaufort, C., Winston, N. J., Sweeney, C., Kubelka, M., Carrington, M., Brechot, C., and Sobczak-Thepot, J. (1997) *Nat. Genet.* **15,** 83–86
37. Brandeis, M., Rosewell, I., Carrington, M., Crompton, T., Jacobs, M. A., Kirk, J., Gannon, J., and Hunt, T. (1998) *Proc. Natl. Acad. Sci. U. S. A.* **95,** 4344–4349
38. Ortega, S., Prieto, I., Odajima, J., Martín, A., Dubus, P., Sotillo, R., Barbero, J. L., Malumbres, M., and Barbacid, M. (2003) *Nat. Genet.* **35,** 25–31
39. Masumoto, H., Muramatsu, S., Kamimura, Y., and Araki, H. (2002) *Nature* **713,** 1–5
40. Pelizon, C., Madine, M. A., Romanowski, P., and Laskey, R. A. (2000) *Genes Dev.* **14,** 2526–2533
41. Higa, L. A. A., Mihaylov, I. S., Banks, D. P., Zheng, J., and Zhang, H. (2003) *Nat. Cell Biol.* **5,** 1008–1015

[CANCER RESEARCH 64, 3545–3549, May 15, 2004]

Expression of a Novel Human Gene, *Human Wings Apart-Like (hWAPL)*, Is Associated with Cervical Carcinogenesis and Tumor Progression

Kosuke Oikawa,[1,3,4] Tetsuya Ohbayashi,[1,3,4] Tohru Kiyono,[5] Hirotaka Nishi,[2] Keiichi Isaka,[2] Akihiro Umezawa,[4,6] Masahiko Kuroda,[1,3,4] and Kiyoshi Mukai[1]

Departments of [1]Pathology and [2]Obstetrics-Gynecology, Tokyo Medical University, Shinjuku-ku, Tokyo; [3]Core Research for Evolutional Science and Technology Research Project, Japan Science and Technology Corp., Kawaguchi-shi, Saitama; [4]Shinanomachi Research Park, Keio University, Shinjuku-ku, Tokyo; [5]Division of Virology, National Cancer Center Research Institute, Chuo-ku, Tokyo; and [6]National Research Institute for Child Health and Development, Setagaya-ku, Tokyo, Japan

ABSTRACT

In *Drosophila melanogaster*, the *wings apart-like* (*wapl*) gene encodes a protein that regulates heterochromatin structure. Here, we characterize a novel human homologue of *wapl* (termed *human WAPL*; *hWAPL*). The *hWAPL* mRNA was predominantly expressed in uterine cervical cancer, with weak expression in all other normal and tumor tissues examined. hWAPL expression in benign epithelia was confined to the basal cell layers, whereas in dysplasias it increasingly appeared in more superficial cell layers and showed a significant correlation with severity of dysplasia. Diffuse hWAPL expression was found in all invasive squamous cell carcinomas examined. In addition, NIH3T3 cells overexpressing hWAPL developed into tumors on injection into nude mice. Furthermore, repression of *hWAPL* expression by RNA interference induced cell death in SiHa cells. These results demonstrate that hWAPL is associated with cell growth, and the *hWAPL* expression may play a significant role in cervical carcinogenesis and tumor progression.

INTRODUCTION

The *wings apart-like* (*wapl*) gene of *Drosophila melanogaster* encodes a protein that regulates heterochromatin structure (1). Mutations of *wapl* prevent the normal close apposition of sister chromatids in heterochromatin regions but do not appear to affect either heterochromatin condensation or chromosomal segregation (1). This evidence suggests that *wapl* is required to hold sister chromatids together in mitotic heterochromatin. *wapl* has also been implicated in both heterochromatin pairing during female meiosis and the modulation of position effect variegation (1). In addition, a *P* element screen of *Drosophila* identified *wapl* as a modifier of chromosome inheritance (2).

Among all varieties of cancer, uterine cervical cancer is unique because of its association with high-risk human papillomavirus (HPV) infection, with strains like HPV-16 and HPV-18. High-risk HPVs encode two oncoproteins, E6 and E7, which subvert crucial cellular regulatory mechanisms that reactivate and maintain DNA synthesis in the host cell. E6 accelerates proteosomal degradation of the p53 tumor suppressor, and E7 inactivates the retinoblastoma protein, interfering with the action of both $p16^{INK4a}$ (3) and the cyclin-dependent kinase inhibitor $p21^{Cip1}$ (4, 5). Both the E6 and E7 high-risk HPV oncoproteins independently induce genomic instability in normal human cells (6, 7). Only a small portion of precursor lesions infected with HPV, however, develops into invasive carcinomas (8). Therefore, additional genetic and microenvironmental factors subsequent to HPV infection are thought to play an important role in the initiation and progression of cervical neoplasia (8–10).

In this study, we describe the isolation and characterization of a novel human *wapl*-related gene termed *human WAPL* (*hWAPL*). We have also demonstrated that *hWAPL* has the characteristics of an oncogene and is associated with uterine cervical cancer.

MATERIALS AND METHODS

cDNA Cloning and Construction of the hWAPL Expression Vector. To isolate the complete *hWAPL* cDNA sequence, we used a human testis Marathon-Ready cDNA kit (Clontech, Palo Alto, CA).

To create an expression vector encoding *hWAPL*, a *Hin*dIII-*Eco*RI cDNA fragment containing the complete coding region of hWAPL was amplified by PCR using the primers 5′-TTAAGCTTTGAAACTGGTGTCAAAATGACATCCAGATT-3′ and 5′-TTGAATTCAAGCAATGTTCCAAATATTCAATCACTCTAGAG-3′ and inserted into the hemagglutinin (HA)-tagged mammalian expression vector, pHM6 (HA-hWAPL; Roche Diagnostics, Mannheim, Germany).

Northern Blot and Quantitative Real-Time PCR Analysis. RNA isolation (11) and Northern blot analysis (11, 12) were performed as described. The 674-bp *Dpn*II fragment of *hWAPL* cDNA was used as a probe and labeled with ^{32}P using the Rediprime II random prime labeling system (Amersham Biosciences, Piscataway, NJ). A human β-actin cDNA control probe (Clontech) was used as a control.

First-strand cDNA synthesis was performed as described (13). Real-time PCR analysis was performed using the Smart Cycler System (Cepheid, Sunnyvale, CA) with SYBR Green I (Cambrex, Washington, DC). Real-time PCR used the *hWAPL*-specific primers 5′-GAATTCATAGGCACAGCGCTGAACTGTGTG-3′ and 5′-TTGAATTCCTAGCAATGTTCCAAATATTCA-3′ and β-actin-specific primers 5′-GGGAAATCGTGCGTGACATTAAG-3′ and 5′-TGTGTTGGCGTACAGGTCTTTG-3′. Reaction mixtures were denatured at 95°C for 30 s and then were subjected to 40 PCR cycles at 95°C for 3 s, 68°C for 30 s, and 87°C for 6 s. *hWAPL* mRNA levels were normalized to β-actin signals.

Immunohistochemistry and Immunoblot Analysis. To generate mouse monoclonal antibodies against hWAPL, we immunized mice against a 6 × histidine-tagged hWAPL COOH terminus (amino acids 814-1037) fusion protein. Spleen cells of an immunized mouse were fused with P3UI mouse myeloma cells as described previously (14). Of the 128 hybrids generated, one clone (clone R929) showed exclusive reactivity with hWAPL by ELISA. We used the supernatant of this clone as anti-hWAPL antibody.

Immunohistochemical assays were performed on formalin-fixed, paraffin-embedded sections using Ventana HX System Benchmark (Ventana Medical Systems Inc., Tucson, AZ). Immunohistochemical stains for hWAPL were interpreted semiquantitatively by assessing the intensity and extent of staining on the entire tissue sections present on the slides as described (9).

Immunoblot analyses were performed as described previously (15). The anti-HA (Roche Diagnostics; 3F10) and monoclonal anti-α-tubulin clone B-5-1-2 (Sigma Chemical Co., St. Louis, MO; T-5168) antibodies were purchased.

Animals and Treatment. BALB/cAJc1-nu female mice (4 weeks old) were purchased from Charles River Japan, Inc. (Kanagawa, Japan).

The tumorigeneicity of the stable NIH3T3 transformants overexpressing hWAPL *in vivo* was examined as described previously (16).

Cell Culture and small interfering RNA (siRNA) Transfection. SiHa and NIH3T3 cells were grown in DMEM (Sigma) containing 10% fetal bovine serum at 37°C in a 5% CO_2 environment. For the transfection of siRNA, we

Received 12/8/03; revised 3/15/04; accepted 3/16/04.

Grant support: Grant-in-Aid for Scientific Research on Priority Area (C) and Grant-in-Aid for Encouragement of Young Scientists from the Ministry of Education, Culture, Sports, Science and Technology, Japan, and a grant from Core Research for Evolutional Science and Technology, Japan Science and Technology Corp.

The costs of publication of this article were defrayed in part by the payment of page charges. This article must therefore be hereby marked *advertisement* in accordance with 18 U.S.C. Section 1734 solely to indicate this fact.

Note: T. Ohbayashi is currently at the Horizontal Medical Research Organization, Kyoto University Faculty of Medicine, Kyoto, Japan.

Requests for reprints: Masahiko Kuroda, Department of Pathology, Tokyo Medical University, 6-1-1, Shinjuku, Shinjuku-ku, Tokyo, 160-8402, Japan. Fax: 81-3-3352-6335; E-mail: kuroda@tokyo-med.ac.jp.

generated siRNAs using a Silencer siRNA Construction Kit (Ambion, Austin, TX). siRNA transfection was performed in DMEM without serum using Oligofectamine Reagent (Invitrogen Japan, Tokyo, Japan) and Opti-MEM I (Invitrogen Japan).

For cell quantitation, we harvested the cells from the wells of a 12-well plate and resuspended them in 100 μl of PBS. Trypan blue solution (100 μl, 0.4%; Sigma) was added to each sample, and viable cell numbers were quantitated using an erythrometer. The results shown are representative of three independent cell count analyses.

RESULTS

Molecular Cloning of *hWAPL*. To isolate *wapl*-related genes from human cells, we searched DNA databases and identified a cDNA fragment, KIAA0261 (17), and three expressed sequence tag clones, BE410177, BF79516, and BE257022, containing the KIAA0261 sequence. We also performed 5′ rapid amplification of cDNA ends. From these DNA sequences, we cloned and confirmed the full-length coding region sequence of the cDNA containing KIAA0261. We named this gene *hWAPL* (GenBank accession no. AB065003) to reflect its homology to *wapl*. The *hWAPL* gene product shows high sequence similarity in the WAPL-conserved region (amino acids 627-1169, 34% identical and 56% similar) and low similarity throughout the other regions to the *wapl* gene product. Several additional stretches of amino acids are also present in wapl protein (Fig. 1*A*).

High-Level Expression of hWAPL in Human Cervical Cancer. As *wapl* is involved in sister chromatid cohesion, hWAPL may modify chromosomal inheritance. Deregulation of the expression of genes involved in chromosomal inheritance directly induces a variety of disorders associated with aneuploidy, including birth defects and cancer. Northern blot analysis detected *hWAPL* mRNA expression in several invasive cervical cancer samples, examined in tandem with additional human cancers and normal tissues (Fig. 1*B*). We confirmed the *hWAPL* expression in cervical cancers by quantitative real-time PCR analysis of tumor and normal tissue samples. The levels of *hWAPL* mRNA expression in cervical cancers were significantly higher than the levels observed in either normal cervical controls or endometrial, ovarian, breast, lung, stomach, renal, and colon cancers (Fig. 1*C*).

To investigate the connection between hWAPL expression and oncogenesis in cervical malignancies, we examined the expression of hWAPL by immunohistochemistry in a series of clinical samples of the various grades of cervical dysplasia [cervical intraepithelial neoplasia (CIN) I–III] and invasive squamous cell carcinoma. We found nuclear immunostaining for hWAPL in all samples (Fig. 2*A*). hWAPL expression in benign squamous epithelia was confined to the basal and parabasal cell layers. In contrast, hWAPL expression in squamous dysplasia and invasive carcinoma increasingly appeared in the more superficial cell layers and was significantly increased compared with the adjacent benign epithelia ($P = 0.0002$ for CIN I, $P = 0.0003$ for CIN II, $P = 0.0001$ for CIN III, and $P = 0.0001$ for invasive squamous cell carcinoma; Wilcoxon's signed rank test). CIN I and II cases showed hWAPL expression in the basal 50 and 70% of the epithelial thickness, respectively, whereas CIN III and invasive squamous cell carcinoma showed hWAPL expression in the full thickness of the dysplastic epithelia (Fig. 2*A*). Furthermore, the mean hWAPL staining score increased remarkably with increasing grade of dysplasia (Fig. 2*B*). These data strongly suggest that the unscheduled high-level expression of hWAPL may play a significant role in cervical carcinogenesis and tumor progression.

hWAPL Has Oncogenic Characteristics. Because we observed high-level expression of *hWAPL* in tumors, we sought to determine whether hWAPL overexpression promotes tumor development. We transfected NIH3T3 cells with an HA-tagged hWAPL expression vector (HA-hWAPL 3T3) or HA expression vector (HA-3T3). Then, we compared the ability of HA-hWAPL 3T3 with HA-3T3 cells to grow as tumors in nude mice. We injected 10^6 cells into three s.c. sites of each nude mouse. HA-hWAPL 3T3 cells produced tumors in all nude mice within 10 days after injection of cells (100%, $n = 18$; Fig. 3*A*). HA-3T3 failed to produce tumors in any mice (0%, $n = 18$). We confirmed high hWAPL expression levels in the resultant tumors by Western blot analysis (Fig. 3*B*). These results suggest that *hWAPL* has the characteristics of an oncogene.

Repression of hWAPL Expression Induces Cell Death. We examined hWAPL function by suppressing hWAPL expression. Initial attempts to generate a *WAPL*-deficient mouse demonstrated that the loss of *WAPL* was embryonic lethal (data not shown). Therefore, we designed two 21-nucleotide, double-stranded siRNAs, siRNA(I) and siRNA(II), to repress *hWAPL* expression (Refs. 18 and 19; Figs. 1*A*

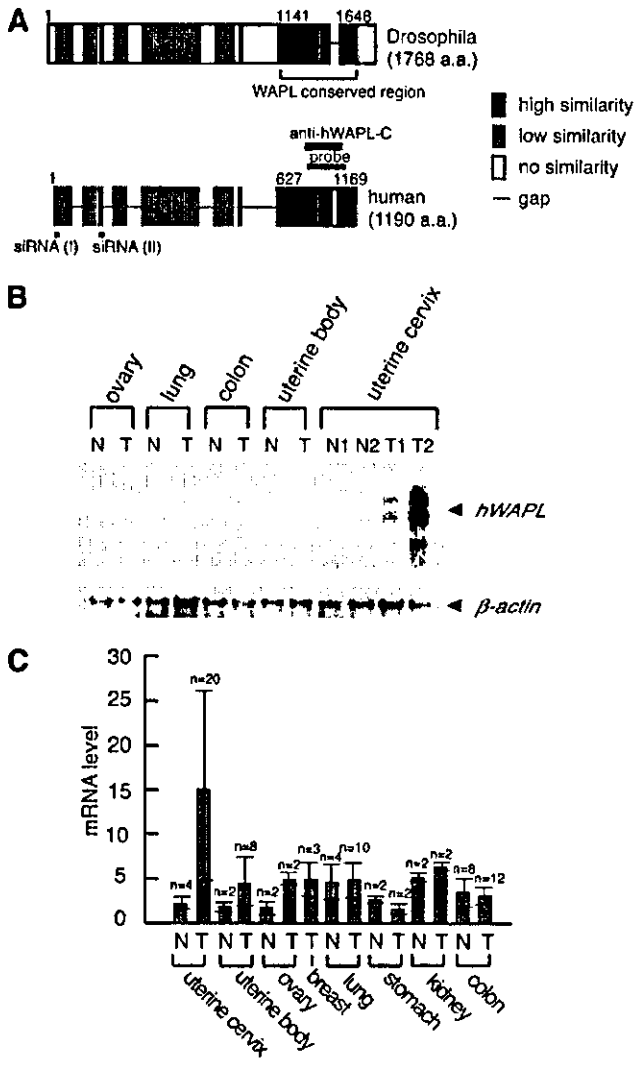

Fig. 1. Structures of wings apart-like (*WAPL*) proteins and *human WAPL* (*hWAPL*) expression in normal and tumor human tissues. *A*, schematic structure of the *hWAPL* and *Drosophila wapl* gene products. The site corresponding to the probe sequence used for Northern blot analysis is indicated by "probe." The antibody recognition site is indicated by "hWAPL-C." The small interfering RNA (*siRNA*) targeting sites are indicated by "siRNA(I)" and "siRNA(II)." *B*, Northern blot analysis of *hWAPL* in several normal (*N*) and tumor (*T*) human tissues. *C*, quantitative real-time PCR analysis demonstrating *hWAPL* mRNA levels in various normal (*N*) and tumor (*T*) human tissues. *Columns*, the means of examined samples. The minimum mRNA expression level was arbitrarily set to 1 in the graphical presentation; all other mRNA signals were normalized to this value. *Bars*, SD.

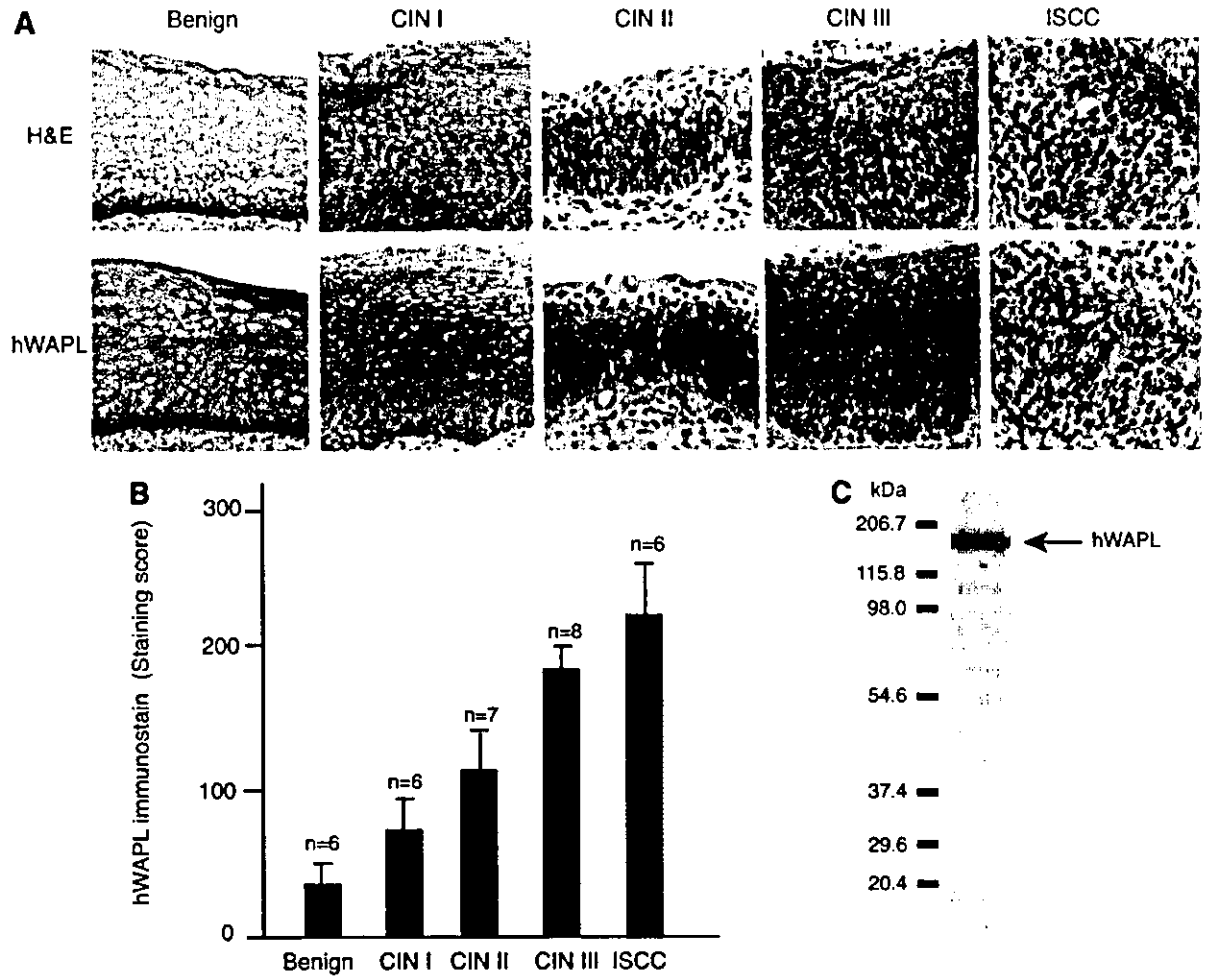

Fig. 2. Immunohistochemical analysis of human wings apart-like (*hWAPL*) expression in uterine cervical epithelia of normal, dysplasia, and carcinoma. *A*, immunohistochemical staining of hWAPL expression in benign squamous epithelium, various grades of squamous dysplasia [cervical intraepithelial neoplasia (*CIN*) grades I, II, and III], and invasive squamous cell carcinoma (*ISCC*). hWAPL was stained with hematoxylin counterstain; H&E. *B*, graphical representation of the increase of the hWAPL expression with increasing severity of dysplasia in cervical squamous epithelia. The mean hWAPL staining scores were calculated as described (9). *Bars*, SD. *C*, Western blot analysis with the total extract from a uterine cervical cancer-derived cell line, SiHa, to confirm the specificity of the anti-hWAPL monoclonal antibody hWAPL-C.

and 4*A*). We examined various human cancer-derived cell lines and found that cervical cancer-derived cell lines containing both HPV-positive and -negative cells exhibited higher levels of hWAPL expression compared with the other cell lines (data not shown). Then, we examined the effects of suppressing *hWAPL* in a cervical cancer-derived cell line, SiHa. siRNA transfection at a concentration of either 1 nM siRNA(I) or siRNA(II) reduced *hWAPL* mRNA levels (Fig. 4*B*). siRNA(I) was more effective at reducing *hWAPL* mRNA than siRNA(II). Thus, we used siRNA(I) in the subsequent experiments. hWAPL protein levels were also significantly reduced after siRNA(I) transfection (Fig. 4*C*). Interestingly, siRNA(I) repressed the growth of the cells and subsequently induced cell death (Fig. 4, *D* and *E*). siRNA(II) repressed cell growth in a similar manner as siRNA(I) (Fig. 4*D*), suggesting that the effects of these siRNAs on proliferation and viability are likely caused by the repression of *hWAPL* expression. Similar results were obtained in another cervical cancer-derived cell line, CaSki, with 10 nM siRNA(I) (data not shown). On the contrary, we did not observe any effects of siRNA(I) on cells expressing relatively low levels of *hWAPL*, such as Saos-2 and HCT116 (data not shown).

To investigate the fate of cells transfected with siRNA(I), we analyzed siRNA-transfected cells by flow cytometry (Fig. 5). In siRNA(I)-transfected cells, the population of cells exhibiting S phase DNA content increased (Fig. 5; 48 and 72 h). In addition, there was an increase in the number of apoptotic cells exhibiting subG$_1$ DNA content (Fig. 5; 72 h). Many cells showing S phase DNA content may also be apoptotic cells at G$_2$-M phase. Taken together, these results suggest that a malfunction in the hWAPL pathway activates an S phase checkpoint or another apoptotic pathway and consequently leads to cell death.

DISCUSSION

In this study, we report the isolation and characterization of a novel human gene termed *hWAPL*. We were unable to identify additional genes similar to *wapl* within the human genome sequence database. Thus, although the high-sequence conservation between hWAPL and wapl is limited to a third of the protein sequence encoded by *wapl* (Fig. 1*A*), we consider hWAPL to be the human homologue of wapl. We did not find any protein sequence motifs in hWAPL, except for the WAPL-conserved region (Fig. 1*A*). We therefore expect that hWAPL has similar functions to the wapl protein. Two hybridization signals for *hWAPL* were visible by Northern blot analysis (Fig. 1*B*). Western blot analysis, however, detected only a single band for

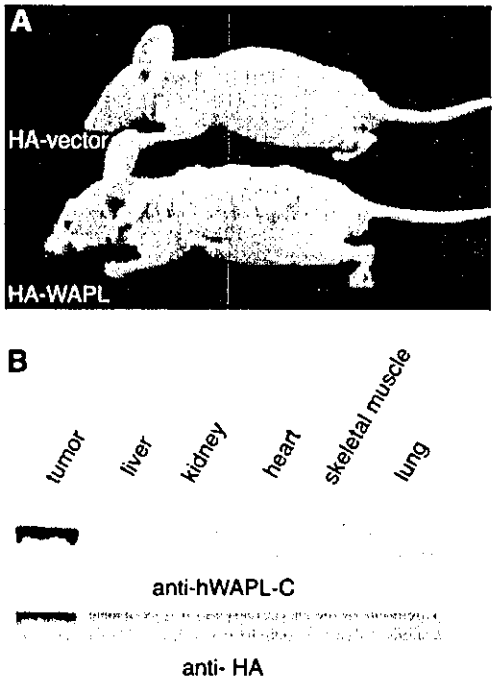

Fig. 3. Human wings apart-like (*hWAPL*) overexpression promotes tumor development. *A*, tumorigenecity of HA-hWAPL 3T3 in nude mice. The lower mouse in the *panel* is shown 10 days after the injection of HA-hWAPL-3T3 at three s.c. sites. The upper mouse was injected with the control HA-3T3 cells. *B*, Western blot analysis of hWAPL protein in tumor and other control tissues from HA-hWAPL-3T3-injected nude mice. *Top panel*, anti-hWAPL antibody; *bottom panel*, anti-HA antibody.

hWAPL (Fig. 2*C*). In addition, we did not obtain additional nucleotide sequences similar to the open reading frame of *hWAPL* by PCR analysis with various PCR primers (data not shown). Thus, we consider that the two hybridization signals may reflect the difference of the length of the untranslated regions of the *hWAPL* mRNA.

High-level expression of *hWAPL* was observed in cervical cancers (Fig. 1, *B* and *C*). Furthermore, hWAPL-overexpressing 3T3 cells developed into tumors on injection into nude mice (Fig. 3). These results suggest that *hWAPL* has oncogenic characteristics. Cervical cancer is a serious health problem, with ~500,000 women developing the disease each year worldwide. In many developing countries, it is the most common cause of cancer death and years of life lost because of cancer (20). Although the fundamental role of high-risk HPV infection in the pathogenesis of cervical carcinoma is well established, other factors are thought to play a role in cervical carcinogenesis (8, 21). Because all of uterine cervical samples examined were HPV positive (data not shown), it is still to be confirmed whether hWAPL expression is inducible by HPV infection. However, HPV-positive normal cervical tissue samples exhibited low hWAPL expression (Fig. 1, *B* and *C* and data not shown), and an HPV-negative, uterine cervical cancer-derived cell line, C33A, showed high hWAPL expression (data not shown). Thus, hWAPL expression is likely to be more closely related with cervical carcinogenesis than HPV infection. Recently, Acs *et al.* (9) found significant correlation among expression of Epo receptor, $p16^{INK4a}$, and *bcl*-2 in benign and dysplastic squamous epithelia. In our results, hWAPL showed similar expression pattern to Epo receptor and $p16^{INK4a}$ in benign and dysplastic cervical squamous epithelia and invasive squamous cell carcinomas (Fig. 2, *A* and *B*). Although we did not find any evidence for hWAPL being involved in hypoxia-inducible Epo signaling, hWAPL may cooperate with the Epo signaling in the progression of cervical neoplasia. These observations indicate that hWAPL overexpression can be used as a useful diagnostic tool in the detection of cervical dysplasia like $p16^{INK4a}$ (22) and Epo receptor (9). In addition, our results provide the necessity to investigate the potential of hWAPL as a cancer therapeutic target.

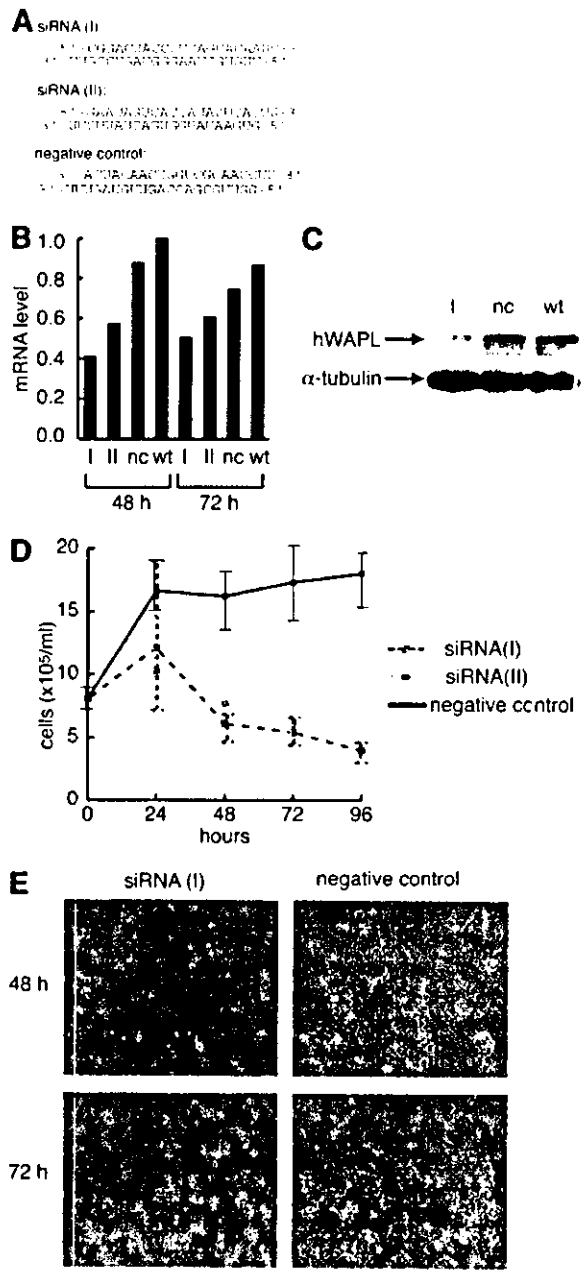

Fig. 4. Repression of human wings apart-like (*hWAPL*) expression by small interfering RNA (*siRNA*) treatment induces cell death. *A*, sequences and structures of siRNAs. The negative control siRNA possesses the same nucleotide composition as siRNA(I) but lacks homology to any known human genes. *B*, reduction of the *hWAPL* transcript by siRNA in SiHa cells. After siRNA transfection, SiHa cells were harvested at either 48 or 72 h. Total RNA was extracted from the cells and subjected to real-time PCR analysis. *I*, siRNA(I); *II*, siRNA(II); *nc*, negative control siRNA; *wt*, untransfected wild type. Data were normalized to a maximum mRNA level that was arbitrarily set to 1 in the graphical presentation. *C*, reduction of hWAPL protein levels by siRNA. Western blot analysis of total cell extracts from untreated SiHa or SiHa cells 72 h after transfection with siRNA(I) or negative control siRNA. α-tubulin is shown as a loading control. *D*, active siRNA specific for *hWAPL* induces cell death. SiHa cells transfected with siRNA(I), siRNA(II), or negative control siRNA were harvested at 24, 48, 72, and 96 h after transfection. Cell numbers were counted using an erythrometer. *Bars*, SE. *E*, representative phase-contrast images of SiHa cells transfected with siRNA(I) and negative control siRNA are shown.

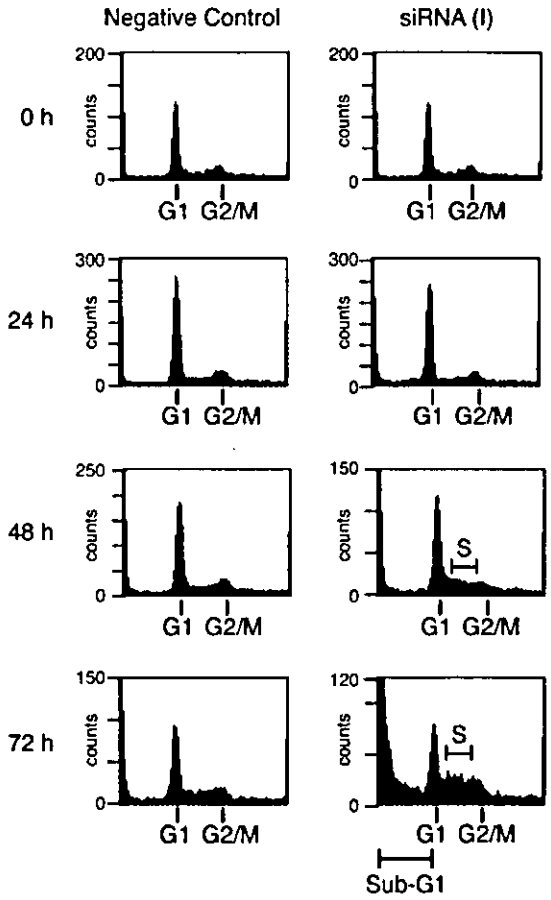

Fig. 5. Flow cytometric analysis of SiHa cells after small interfering RNA (*siRNA*) transfection. SiHa cells were transfected with either siRNA(I) or negative control siRNA, then harvested at 24, 48, and 72 h after transfection. Cells were stained with propidium iodide and subjected to flow cytometric analysis to examine DNA content. A total of 50,000 cells was counted for the sample siRNA(I) 72 h, and 20,000 cells were counted for the other samples.

Loss of WAPL was embryonic lethal in mouse (data not shown), and repression of hWAPL expression in SiHa cells led to cell death (Fig. 4). Flow cytometry analysis demonstrated that malfunction of hWAPL may cause apoptosis and/or arrest of cells at S phase (Fig. 5). In addition, *Drosophila wapl* is associated with regulation of chromatin organization (1). Thus, we expect that hWAPL is also associated with regulation of chromatin structure, and deregulation of hWAPL expression may induce chromosomal instability. Although additional investigations are necessary to elucidate the actual function of hWAPL in normal and malignant cells, our results have demonstrated that the novel oncogene, *hWAPL*, is one of the essential genes for development and cell growth and may play a significant role for cervical carcionogenesis and tumor progression.

ACKNOWLEDGMENTS

We thank K. Yoshida, R. Iwata, R. Tsujimoto, K. Kitamura, M. Sugiura, and M. Takaoka for their technical assistance.

REFERENCES

1. Verni F, Gandhi R, Goldberg ML, Gatti M. Genetic and molecular analysis of wings apart-like (wapl), a gene controlling heterochromatin organization in Drosophila melanogaster. Genetics 2000;154:1693–710.
2. Dobie KW, Kennedy CD, Velasco VM, et al. Identification of chromosome inheritance modifiers in Drosophila melanogaster. Genetics 2001;157:1623–37.
3. Kiyono T, Foster SA, Koop JI, McDougall JK, Galloway DA, Klingelhutz AJ. Both Rb/p16^{INK4a} inactivation and telomerase activity are required to immortalize human epithelial cells. Nature 1998;396:84–8.
4. Jones DL, Alani RM, Munger K. The human papillomavirus E7 oncoprotein can uncouple cellular differentiation and proliferation in human keratinocytes by abrogating p21^{Cip1}-mediated inhibition of cdk2. Genes Dev 1997;11:2101–11.
5. zur Hausen H. Papillomavirus infections–a major cause of human cancers. Biochim Biophys Acta 1996;1288:F55–78.
6. Hashida T, Yasumoto S. Induction of chromosome abnormalities in mouse and human epidermal keratinocytes by the human papillomavirus type 16 E7 oncogene. J Gen Virol 1991;72:1569–77.
7. White AE, Livanos EM, Tlsty TD. Differential disruption of genomic integrity and cell cycle regulation in normal human fibroblasts by the HPV oncoproteins. Genes Dev 1994;8:666–77.
8. Milde-Langosch K, Riethdorf S, Loning T. Association of human papillomavirus infection with carcinoma of the cervix uteri and its precursor lesions: theoretical and practical implications. Virchows Arch 2000;437:227–33.
9. Acs G, Zhang PJ, McGrath CM, et al. Hypoxia-inducible erythropoietin signaling in squamous dysplasia and squamous cell carcinoma of the uterine cervix and its potential role in cervical carcinogenesis and tumor progression. Am J Pathol 2003; 162:1789–806.
10. Schiffman MH, Brinton LA. The epidemiology of cervical carcinogenesis. Cancer 1995;76:1888–901.
11. Oikawa K, Ohbayashi T, Mimura J, et al. Dioxin suppresses the checkpoint protein, MAD2, by an aryl hydrocarbon receptor-independent pathway. Cancer Res 2001;61: 5707–9.
12. Sok J, Wang XZ, Batchvarova N, Kuroda M, Harding H, Ron D. CHOP-dependent stress-inducible expression of a novel form of carbonic anhydrase VI. Mol Cell Biol 1999;19:495–504.
13. Kuroda M, Ishida T, Takanashi M, Satoh M, Machinami R, Watanabe T. Oncogenic transformation and inhibition of adipocytic conversion of preadipocytes by TLS/FUS-CHOP type II chimeric protein. Am J Pathol 1997;151:735–44.
14. Kuroda M, Horiuchi H, Ono A, Kawakita M, Oka T, Machinami R. Immunohistochemical study on the distribution of sarcoplasmic reticulum calcium ATPase in various human tissues using novel monoclonal antibodies. Virchows Arch A Pathol Anat Histopathol 1992;421:527–32.
15. Oikawa K, Ohbayashi T, Mimura J, et al. Dioxin stimulates synthesis and secretion of IgE-dependent histamine-releasing factor. Biochem Biophys Res Commun 2002; 290:984–7.
16. Kuroda M, Wang X, Sok J, et al. Induction of a secreted protein by the myxoid liposarcoma oncogene. Proc Natl Acad Sci USA 1999;96:5025–30.
17. Nagase T, Seki N, Ishikawa K, et al. Prediction of the coding sequences of unidentified human genes. VI. The coding sequences of 80 new genes (KIAA0201-KIAA0280) deduced by analysis of cDNA clones from cell line KG-1 and brain. DNA Res 1996;3:321–9, 41–54.
18. Hannon GJ. RNA interference. Nature 2002;418:244–51.
19. McManus MT, Sharp PA. Gene silencing in mammals by small interfering RNAs. Nat Rev Genet 2002;3:737–47.
20. Waggoner SE. Cervical cancer. Lancet 2003;361:2217–25.
21. Park TW, Fujiwara H, Wright TC. Molecular biology of cervical cancer and its precursors. Cancer 1995;76:1902–13.
22. Klaes R, Friedrich T, Spitkovsky D, et al. Overexpression of p16^{INK4a} as a specific marker for dysplastic and neoplastic epithelial cells of the cervix uteri. Int J Cancer 2001;92:276–84.

Cell Death and Differentiation (2004) 11, 853–861

www.nature.com/cdd

p53-Independent ceramide formation in human glioma cells during γ-radiation-induced apoptosis

S Hara*,[1], S Nakashima[2], T Kiyono[3], M Sawada[1], S Yoshimura[1], T Iwama[1], Y Banno[2], J Shinoda[1] and N Sakai[1]

[1] Department of Neurosurgery, Gifu University School of Medicine, Tsukasamachi-40, Gifu 500-8705, Japan;
[2] Department of Cell Signaling, Division of Cellular and Molecular Biology, Gifu University School of Medicine, Tsukasamachi-40, Gifu 500-8705, Japan;
[3] Virology Division, National Cancer Center Research Institute, 5-1-1 Tsukiji, Chuohku, Tokyo 104-0045, Japan
* Corresponding author: S Hara, Department of Neurosurgery, Gifu University School of Medicine, Tsukasamachi-40, Gifu 500-8705, Japan.
Tel: +81-58-267-2348; Fax: +81-58-265-9025;
E-mail: f2105013@guedu.cc.gifu-u.ac.jp

Received 22.7.03; revised 15.1.04; accepted 10.2.04; published online 16.4.04
Edited by D Altieri

Abstract

Although the p53 tumor-suppressor gene product plays a critical role in apoptotic cell death induced by DNA-damaging chemotherapeutic agents, human glioma cells with functional p53 were more resistant to γ-radiation than those with mutant p53. U-87 MG cells with wild-type p53 were resistant to γ-radiation. U87-W E6 cells that lost functional p53, by the expression of type 16 human papillomavirus E6 oncoprotein, became susceptible to radiation-induced apoptosis. The formation of ceramide by acid sphingomyelinase (A-SMase), but not by neutral sphingomyelinase, was associated with p53-independent apoptosis. SR33557 (2-isopropyl-1-(4-[3-*N*-methyl-*N*-(3,4-dimethoxybphenethyl)amino]propyloxy)benzene-sulfonyl) indolizine, an inhibitor of A-SMase, suppressed radiation-induced apoptotic cell death. In contrast, radiation-induced A-SMase activation was blocked in glioma cells with endogenous functional p53. The expression of acid ceramidase was induced by γ-radiation, and was more evident in cells with functional p53. *N*-oleoylethanolamine, which is known to inhibit ceramidase activity, unexpectedly downregulated acid ceramidase and accelerated radiation-induced apoptosis in U87-W E6 cells. Moreover, cells with functional p53 could be sensitized to γ-radiation by *N*-oleoylethanolamine, which suppressed radiation-induced acid ceramidase expression and then enhanced ceramide formation. Sensitization to γ-radiation was also observed in U87-MG cells depleted of functional p53 by retroviral expression of small interfering RNA. These results indicate that ceramide may function as a mediator of p53-independent apoptosis in human glioma cells in response to γ-radiation, and suggest that p53-dependent expression of acid ceramidase and blockage of A-SMase activation play pivotal roles in protection from γ-radiation of cells with endogenous functional p53.

Cell Death and Differentiation (2004) **11**, 853–861.
doi:10.1038/sj.cdd.4401428
Published online 16 April 2004

Keywords: apoptosis; p53; glioma; radiation; ceramide

Abbreviations: N- and A-SMase, neutral- and acid- sphingomyelinase; SM, sphingomyelin; HPV-16, type 16 human papillomavirus; GADD45, growth arrest and DNA-damage-inducible gene 45; OE, *N*-(*cis*-9-octadecenoyl)ethanol-amine (*N*-oleoylethanolamine); SR33557, (2-isopropyl-1-(4-[3-*N*-methyl-*N*-(3,4-dimethoxybphenethyl)amino]propyloxy)benzene-sulfonyl) indolizine; TNF, tumor necrosis factor; SPP, sphingosine-1-phosphate; DMEM, Dulbecco's modified Eagle's medium; FBS, fetal bovine serum; PBS, phosphate-buffered saline; MTT, 3-(4,5-dimethyl-2-thiazolyl)-2, 5-diphenyl-2H-tetrazolium bromide (methylthiazoletetrazolium); siRNA, small interfering RNA; shRNA, short hairpin RNA; HPTLC, high-performance thin-layer chromatography; SDS–PAGE, sodium dodecylsulfate polyacrylamide gel electrophoresis

Introduction

Malignant gliomas, the most common malignant brain tumors, are usually incurable. While radiation therapy is the most effective postoperative adjuvant treatment, it does not substantially alter long-term outcomes[1] due to the characteristic *in vivo* and *in vitro* radioresistance of these tumors.[2] The underlying molecular mechanism(s) of their radioresistance and the radiation-induced apoptotic death of glioma cells remain poorly understood. DNA-damaging agents, used to treat malignant tumors, induce tumor cell apoptosis.[3] Caspases, a family of cysteine proteases, play a central role in the apoptotic cascade.[4] Ceramide, a product of the sphingomyelinase (SMase)-catalyzed hydrolysis of sphingomyelin (SM), is closely implicated in the apoptosis of several types of cells.[5] We previously reported the molecular mechanism by which etoposide, an anticancer drug, induces ceramide generation in human glioma cells.[6–8] However, the role of ceramide in radiation-induced apoptosis in gliomas remains to be clarified.

Chemotherapeutic agents upregulate and activate p53, a tumor-suppressor gene product. p53 protein is a prerequisite for cell-cycle arrest in the repair of damaged DNA, or alternatively, for the promotion of apoptosis, when DNA damage is too extreme.[9] p53 stimulates transcriptional activation to regulate as many as 200–400 gene products involved in cell-cycle control ($p21^{WAF1}$), DNA repair and synthesis (GADD45, growth-arrest and DNA-damage-inducible gene 45), and apoptosis (Bax and Apaf-1).[10,11] Cells with functional p53 or exogenously expressed p53 are usually more sensitive to chemotherapeutic agents such as etoposide than are cells with mutant p53.[8,12,13] Supraphysiological levels of p53, such as those generated by adenovirus delivery, trigger apoptosis in glioma cell lines containing the mutant p53,[14] and enhance the radiosensitivity of glioma cells with wild-type p53.[15–17] However, the role of endogenous p53 in radiation-induced apoptosis of glioma cells remains to be elucidated. Glioma cells with p53 mutations are reportedly

more sensitive to γ-radiation than those with endogenous wild-type (functional) p53.[18,19] Endogenous functional p53 mediates radiation-induced G_1 arrest rather than apoptosis.[18] These results point to p53-independent apoptosis of glioma cells with p53 mutations, although the apoptotic signaling pathway(s) remains understood. However, Badie *et al*.[16] reported that radiation did not induce significant apoptosis in glioma cells regardless of their p53 status.

In the present study, we evaluated the involvement of endogenous p53 in the radiation sensitivity of glioma cells, and examined the pathway(s) of p53-independent apoptosis. Functional p53 was inactivated with the E6 protein of human papillomavirus type 16 (HPV-16).[20] We found that gliomas with endogenous functional p53 were relatively resistant to γ-radiation and that the loss of functional p53 rendered them susceptible to γ-radiation-induced apoptosis. We confirmed our results in glioma cells depleted of p53 by a small interfering RNA (siRNA) technique,[21] which uses retroviral expression of short hairpin RNA (shRNA). In the p53-independent apoptotic pathway, ceramide, produced by acid SMase (A-SMase), appeared to function as a mediator. Furthermore, upregulation of acid ceramidase and blockage of A-SMase activation, which synergistically inhibit the formation of ceramide, may play an important role in the radioresistance of glioma cells with endogenous functional p53.

Results

Sensitivity to γ-radiation based on the p53 status of human glioma cells

We first examined the cytotoxic effects of γ-radiation on two human glioma cell lines of different p53 status. U-373 MG cells with mutant (nonfunctional) p53 were more sensitive to γ-radiation than U-87 MG cells with wild-type (functional) p53 (Figure 1a). Under a phase-contrast microscopy, U-373 MG cells did, while U-87 MG cells did not, manifest marked morphological changes at 72 h after 25 Gy irradiation.

To confirm the role of endogenous p53 in the radiosensitivity of human glioma cells, functional p53 was inactivated by the expression of HPV-16 E6 oncoprotein, which binds p53 and accelerates its proteolytic degradation via the ubiquitin pathway.[20] Using a retroviral vector, wild-type or mutant E6 proteins[22] and an empty vector were expressed in U-87 MG cells (designated U87-W E6, U87-M E6, and U87-LXSN, respectively).[8] γ-Radiation induced the accumulation of p53 protein at 6 h after γ-radiation, thereafter the accumulated p53 was gradually degraded in U87-LXSN and U87-M E6 cells. In contrast, γ-radiation-induced p53 expression was abolished in U87-W E6 cells with wild-type E6 protein (Figure 2a). The accumulation of p53-inducible proteins,[10] $p21^{WAF1}$ and GADD45, was almost completely suppressed in U87-W E6 cells (Figure 2b); thus, p53 was virtually inactivated by E6 protein in these cells.

Exposure to γ-radiation induced time- and dose-dependent increases in apoptosis (Figure 1). U87-W E6 cells were more sensitive to γ-radiation than U87-LXSN and U87-M E6 cells; the latter were almost completely resistant to γ-radiation. Nuclear staining of U87-W E6 cells with Hoechst 33258

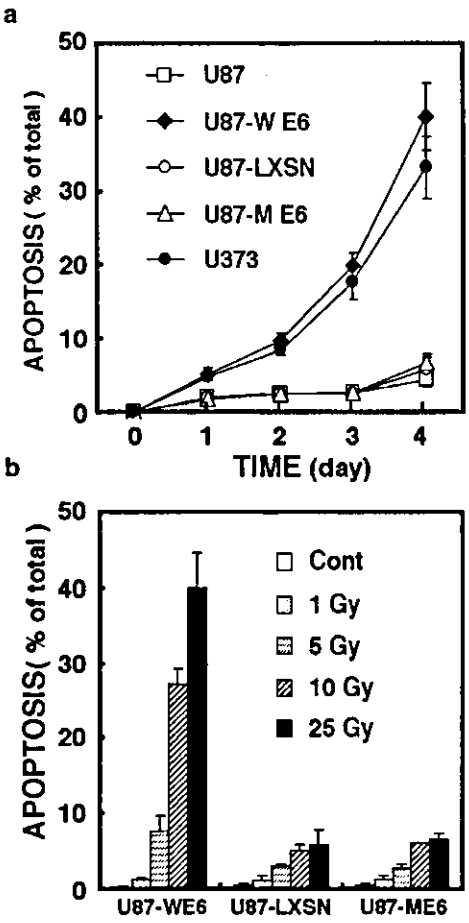

Figure 1 Radiation-induced apoptosis of human glioma cells with different p53 status. (a) U-87 MG, U87-LXSN, U87-W E6, U87-M E6, and U-373 MG cells were irradiated at 25 Gy, and cultured for the indicated periods. (b) U87-LXSN, U87-W E6, and U87-M E6 cells were exposed to the indicated doses of γ-radiation and incubated for 4 days. The cells with fragmented and condensed nuclei were counted in over 1000 cells under a fluorescent microscope. Data are means ± S.D. from three independent experiments, each performed in triplicate

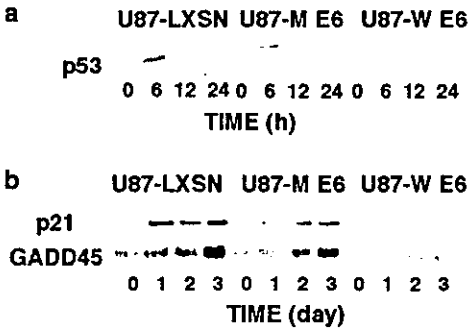

Figure 2 Radiation-induced accumulation of (a) p53 and (b) p53-dependent proteins, $p21^{WAF1}$, and GADD45. U87-LXSN, U87-M E6, and U87-W E6 cells were irradiated at 25 Gy, and incubated for the indicated periods. Cellular proteins were subjected to SDS-PAGE and immunoblotted with antibodies against p53, $p21^{WAF1}$, or GADD45. Results are representative of three separate experiments with compatible outcomes

revealed typical apoptotic changes such as condensation and fragmentation of the nuclei (data not shown). Apoptotic cell death was also confirmed by the activation of caspases-3 and -9. U87-LXSN and U87-M E6 cells manifested hardly any typical apoptotic changes or activation of caspases (data not shown).

Differences in the radiosensitivity of glioma cells with and without endogenous functional p53 were assessed with a clonogenic assay for survival (Figure 3). The clonogenic survival of U87-W E6 cells was significantly lower than that of U87-LXSN and U87-M E6 cells, which possess p53, indicating that functional p53 confers resistance to γ-radiation-induced apoptosis. Our observations are consistent with those of Haas-Kogan *et al.*,[18] who proposed that endogenous functional p53 mediates the radiation-induced G_1 arrest of glioma cells rather than apoptosis.

Formation of ceramide via activation of A-SMase in the course of γ-radiation-induced glioma cell death

Intracellular ceramide levels following γ-radiation were measured by enzymatic analysis using *Escherichia coli* diacylglycerol kinase and by metabolic labeling of cells with [^{14}C]palmitic acid.[6,8] The ceramide level in U87-W E6 cells increased on day 2 and peaked at three times the control level on day 3 (Figure 4a). A similar [^{14}C]ceramide formation profile was obtained for cells labeled with [^{14}C]palmitic acid (data not shown). The ceramide levels of γ-irradiated U87-LXSN cells were above the nonirradiated controls (Figure 4b), but the increase was not statistically significant. γ-Radiation gave rise to an increase in A-SMase– but not N-SMase activity on day 1; this activity peaked on day 3 in U87-W E6 cells. No significant changes in A-SMase activity were noted in U87-LXSN and U87-M E6 cells (Figure 5). These results suggest that functional p53 negatively regulates A-SMase activation

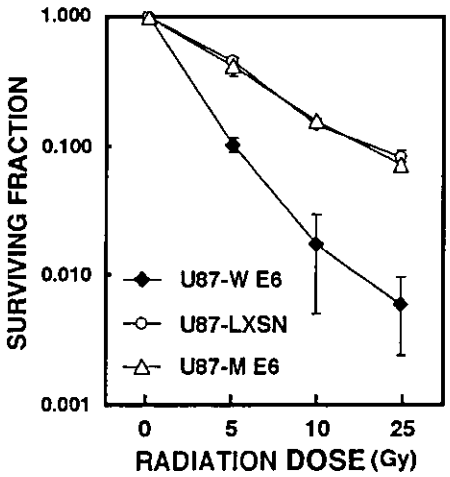

Figure 3 Clonogenic survival after γ-radiation. U87-LXSN, U87-M E6, and U87-W E6, cells were γ-irradiated at the indicated doses, and cultured for 3 days. The cells were then trypsinized, and replated into 100-mm dishes. After incubation for 2 weeks, dishes were stained with trypan blue and colonies with over 50 cells were counted. Data are means ± S.D. from three independent experiments, each performed in triplicate

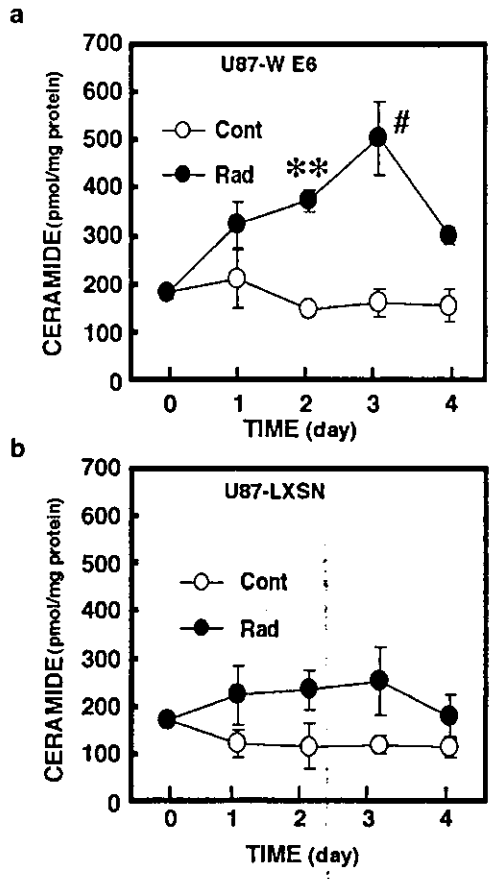

Figure 4 Radiation-induced ceramide formation in (a) U87-W E6 and (b) U87-LXSN cells. The cells were irradiated at 25 Gy (Rad), and cultured for the indicated periods. Ceramide content was measured by the *E. coli* diacylglycerol kinase assay. Data are means ± S.D. from three independent experiments, each performed in triplicate. $^{**}P<0.05$, $^{*}P<0.1$ *versus* nonirradiated control (Cont): two-way ANOVA followed by Scheffe's *post hoc* test

triggered by γ-radiation. To further examine the role of A-SMase in γ-radiation-induced apoptosis, we used SR33557 (2-isopropyl-1-(4-[3-*N*-methyl-*N*-(3,4-dimethoxybphenethyl)amino]propyloxy)benzene-sulfonyl) indolizine, a potent inhibitor of A-SMase activation by various stimuli.[23,24] As shown in Table 1, SR33557 prevented γ-radiation-induced activation of A-SMase in U87-W E6 cells below the control level, but had no effect on N-SMase activity. In fact, it suppressed [^{14}C]ceramide formation in [^{14}C]palmitic acid-labeled U87-W E6 cells (Figure 6a). The number of apoptotic U87-W E6 cells with typical apoptotic features such as condensation and fragmentation of nuclei was suppressed by SR33557 (Figure 6b). Our finding that SR33557 inhibits apoptosis was supported by 3-(4,5-Dimethyl-2-thiazolyl)-2,5-diphenyl-2H-tetrazolium bromide (methylthiazoletetrazolium; MTT) assay results that showed an increase in viable cells.

Change in acid ceramidase

Overexpression of acid ceramidase protects cells from tumor necrosis factor-α (TNF-α)-induced cell death.[25] We found that

revealed typical apoptotic changes such as condensation and fragmentation of the nuclei (data not shown). Apoptotic cell death was also confirmed by the activation of caspases-3 and -9. U87-LXSN and U87-M E6 cells manifested hardly any typical apoptotic changes or activation of caspases (data not shown).

Differences in the radiosensitivity of glioma cells with and without endogenous functional p53 were assessed with a clonogenic assay for survival (Figure 3). The clonogenic survival of U87-W E6 cells was significantly lower than that of U87-LXSN and U87-M E6 cells, which possess p53, indicating that functional p53 confers resistance to γ-radiation-induced apoptosis. Our observations are consistent with those of Haas-Kogan *et al.*,[18] who proposed that endogenous functional p53 mediates the radiation-induced G_1 arrest of glioma cells rather than apoptosis.

Formation of ceramide via activation of A-SMase in the course of γ-radiation-induced glioma cell death

Intracellular ceramide levels following γ-radiation were measured by enzymatic analysis using *Escherichia coli* diacylglycerol kinase and by metabolic labeling of cells with [^{14}C]palmitic acid.[6,8] The ceramide level in U87-W E6 cells increased on day 2 and peaked at three times the control level on day 3 (Figure 4a). A similar [^{14}C]ceramide formation profile was obtained for cells labeled with [^{14}C]palmitic acid (data not shown). The ceramide levels of γ-irradiated U87-LXSN cells were above the nonirradiated controls (Figure 4b), but the increase was not statistically significant. γ-Radiation gave rise to an increase in A-SMase– but not N-SMase activity on day 1; this activity peaked on day 3 in U87-W E6 cells. No significant changes in A-SMase activity were noted in U87-LXSN and U87-M E6 cells (Figure 5). These results suggest that functional p53 negatively regulates A-SMase activation

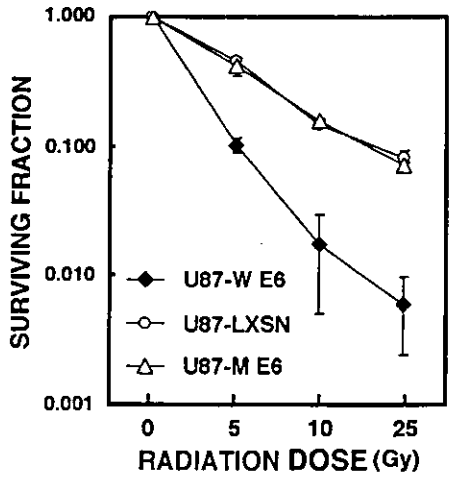

Figure 3 Clonogenic survival after γ-radiation. U87-LXSN, U87-M E6, and U87-W E6, cells were γ-irradiated at the indicated doses, and cultured for 3 days. The cells were then trypsinized, and replated into 100-mm dishes. After incubation for 2 weeks, dishes were stained with trypan blue and colonies with over 50 cells were counted. Data are means ± S.D. from three independent experiments, each performed in triplicate

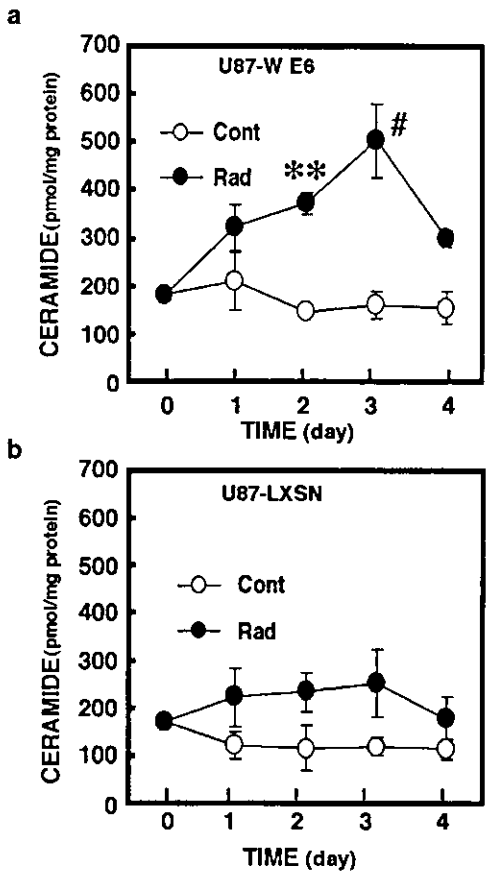

Figure 4 Radiation-induced ceramide formation in (a) U87-W E6 and (b) U87-LXSN cells. The cells were irradiated at 25 Gy (Rad), and cultured for the indicated periods. Ceramide content was measured by the *E. coli* diacylglycerol kinase assay. Data are means ± S.D. from three independent experiments, each performed in triplicate.** $P<0.05$, * $P<0.1$ *versus* nonirradiated control (Cont): two-way ANOVA followed by Scheffe's *post hoc* test

triggered by γ-radiation. To further examine the role of A-SMase in γ-radiation-induced apoptosis, we used SR33557 (2-isopropyl-1-(4-[3-*N*-methyl-*N*-(3,4-dimethoxybphenethyl)amino]propyloxy)benzene-sulfonyl) indolizine, a potent inhibitor of A-SMase activation by various stimuli.[23,24] As shown in Table 1, SR33557 prevented γ-radiation-induced activation of A-SMase in U87-W E6 cells below the control level, but had no effect on N-SMase activity. In fact, it suppressed [^{14}C]ceramide formation in [^{14}C]palmitic acid-labeled U87-W E6 cells (Figure 6a). The number of apoptotic U87-W E6 cells with typical apoptotic features such as condensation and fragmentation of nuclei was suppressed by SR33557 (Figure 6b). Our finding that SR33557 inhibits apoptosis was supported by 3-(4,5-Dimethyl-2-thiazolyl)-2,5-diphenyl-2H-tetrazolium bromide (methylthiazoletetrazolium; MTT) assay results that showed an increase in viable cells.

Change in acid ceramidase

Overexpression of acid ceramidase protects cells from tumor necrosis factor-α (TNF-α)-induced cell death.[25] We found that

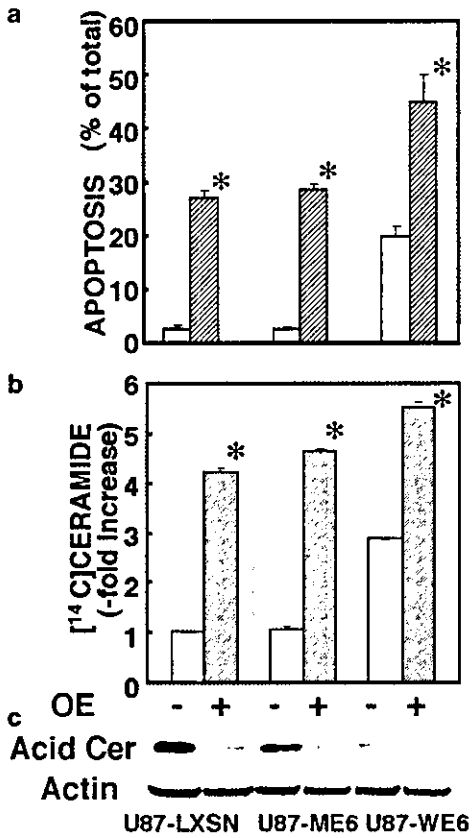

Figure 8 Effects of OE on radiation-induced apoptosis and ceramide formation. U87-LXSN, U87-M E6, and U87-W E6 cells were preincubated without or with 25 μM OE for 24 h, and then were irradiated at 25 Gy. (**a**) The cells with fragmented and condensed nuclei, stained with Hoechst 33258, were counted in over 1000 cells under a fluorescent microscope 3 days after γ-radiation. (**b**) Formation of [^{14}C]ceramide in [^{14}C]palmitic acid-labeled cells was determined at day 3 after γ-radiation. The radioactivity in [^{14}C]ceramide of U87-LXSN without OE was designed as control. Data are means $\pm$ S.D. from three independent experiments. *$P<0.01$ *versus* γ-radiation alone: two-way ANOVA followed by Scheffe's *post hoc* test. (**c**) Cellular proteins were subjected to SDS-PAGE and immunoblotted with antibodies against acid ceramidase or actin (reference control). Results are representative of three separate experiments with compatible outcomes

Depletion of functional p53 by retroviral expression of shRNA specific for p53 sensitizes human glioma cells to γ-radiation-induced apoptosis

Wild-type HPV-16 E6 protein, but not mutant E6 protein, sensitized radiation-resistant U87-MG cells with wild-type p53, suggesting a role for p53 in radiation resistance. However, like p53, HPV-16 E6 protein modulates a variety of proteins involved in important cellular functions.[27–31] As another approach to silencing p53, we employed a siRNA technique[21] that uses retroviral delivery of shRNA. The γ-radiation-induced accumulation of p53 and p53-dependent proteins, such as p21^{WAF1} and GADD45, was abrogated in U87-MG cells infected with retrovirus expressing p53 shRNA (designated U87-p53SI) compared to backbone vector (U87-Vec) (Figure 9a and b). Therefore, p53 was successfully knocked down by this technique. As was the case when

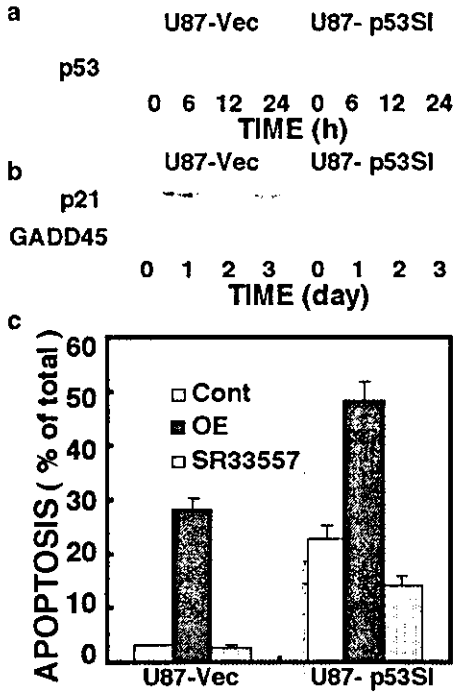

Figure 9 Sensitization to γ-radiation in cells depleted of functional p53 by retroviral expression of shRNA. U-87 MG cells transduced with SI-MSCVpuro-H1R-p53Ri (designed as U87-p53SI) and SI-MSCVpuro-H1R (U87-Vec) were irradiated at 25 Gy, and incubated for the indicated periods. (**a** and **b**) Cellular proteins were subjected to SDS-PAGE and immunoblotted with antibodies against p53, p21^{WAF1}, and GADD45. Data are representative of three separate experiments with compatible outcomes. (**c**) The cells preincubated with 5 μM SR33557 for 6 h or with 25 μM OE for 24 h were irradiated at 25 Gy, and incubated for 3 days. The cells with fragmented and condensed nuclei were counted in over 1000 cells under a fluorescent microscope. Data are means $\pm$ S.D. from three independent experiments, each performed in duplicate

functional p53 was disrupted by HPV-16 E6 retroviral infection, U87-Vec and U87-p53SI cells differed in their radiosensitivity: U87-p53SI cells lacking p53 became sensitive to γ-radiation, while U87-Vec cells that possessed wild-type p53 were radiation resistant (Figure 9c). SR33557, an inhibitor of A-SMase, suppressed γ-radiation-induced apoptosis of U87-p53SI cells. In contrast, OE accelerated the radiation-induced death of U87-p53SI and U87-Vec cells. These results confirm the role of ceramide formed by A-SMase during γ-radiation-induced apoptosis.

Discussion

Wild-type p53 protein can transcriptionally activate genes involved in cell-cycle arrest, DNA repair and synthesis, or apoptosis.[10] In a normal cell, p53-dependent cell-cycle arrest allows enough time for DNA damaged by agents to be repaired. If the damage is beyond repair, p53-dependent apoptosis occurs to prevent transfer of new mutations to daughter cells.[9] Thus, wild-type p53 has been shown to suppress cell transformation and to induce apoptosis in several types of tumors. Adenovirus-mediated delivery of *p53* gene caused apoptosis in glioma cell lines containing mutant *p53* gene.[14] However, in response to exogenous

delivery of supraphysiological levels of p53, glioma cells with wild-type p53 did not undergo apoptosis,[14] but showed a slower growth rate and became sensitive to radiation-induced apoptosis.[15–17] These results indicate that the function of p53 is under strict control, which depends on cellular conditions, and that p53 alone, even at supraphysiological levels, cannot trigger apoptotic signaling pathway.

In the present study, we first attempted to investigate the involvement of endogenous p53 in the radiation sensitivity of glioma cells. We found U-373 MG human glioma cells possessing mutant (nonfunctional) p53 to be more sensitive to γ-irradiation than U-87 MG human glioma cells with wild-type (functional) p53. To confirm these observations, we generated U87-W E6 cells depleted of p53 by HPV-16 E6 protein,[20] as an isogenic clonal derivative of U-87 MG cells. In response to γ-radiation, accumulation of p53 protein and p53-inducible proteins[10] such as $p21^{WAF1}$ and GADD45 was observed in vector-infected U87-LXSN cells and U87-M E6 cells infected with mutant E6 proteins.[21] In contrast, γ-radiation-induced expression of p53 itself and p53-inducible proteins was abolished in U87-W E6 cells. Therefore, endogenous p53 was successfully eliminated by HPV-16 E6 protein in U87-W E6 cells. Typical apoptotic changes, including nuclear morphological changes and activation of caspases at 96 h (4 days) after γ-irradiation, were observed in U87-W E6 cells, but scarcely in U87-LXSN and U87-M E6 cells. The difference in radiation sensitivity between glioma cells with and without endogenous functional p53 was confirmed by clonogenic assay for survival. Since recent studies[27–31] have identified a number of additional cellular targets of HPV-16 E6 protein, we also downregulated p53 by means of siRNA. U87-p53SI cells in which p53 was effectively knocked down, became susceptible to γ-radiation-induced apoptosis. These results suggest that glioma cells without functional p53 are more sensitive to γ-radiation than those with wild-type p53, and are consistent with the results reported by Haas-Kogan *et al.*,[18] who proposed that endogenous functional p53 mediated radiation-induced G_1 arrest rather than apoptosis. It may be reasonable to speculate that p53-dependent induction of $p21^{WAF1}$ observed in Figure 2 takes part in radiation-induced G_1 arrest. Our present observations are, however, inconsistent with the report by Badie *et al.*,[16] that radiation induces significant apoptosis neither in U-373 MG cells with mutant p53 nor in U-87 MG cells possessing functional p53. This discrepancy may be due to differences in the time that elapsed between the γ- radiation and examination, the γ-radiation doses, or the method used to detect apoptosis. They measured apoptosis only 48 h after γ-radiation, whereas we measured it for 4 days and Haas-Kogan *et al.* measured it for 8 days,[18] and they did not observe kinetic changes. In addition, their radiation dose was lower than that of ours. In our kinetic analysis (Figure 1a), at 48 h (2 days) after γ-irradiation, the number of apoptotic U87-W E6 cells was less than 10%, but it reached nearly 40% at 4 days. Therefore, we believe that they would have been able to detect differences between U-373 MG cells and U-87 MG cells after longer incubation periods. Taken together, our results indicate that p53-independent apoptotic signaling pathways operate in γ-irradiated glioma cells, and that endogenous functional p53 may counteract these signals.We next examined the involvement of ceramide in p53-independent apoptotic pathway. Ceramide has been shown to exert potent proapoptotic effects in a variety of cell types.[5] Ceramide is mainly produced from SM by the action of N-SMase and/or A-SMase during apoptosis. N-SMase has been implicated in apoptosis induced by serum starvation,[32] hypoxia,[33] nitric oxide,[34] and some chemotherapeutic agents.[6,35] In glioma cells treated with etoposide, activation of N-SMase occurred downstream of p53-mediated ROS formation.[8] In contrast, A-SMase has been suggested to be activated in cells exposed to radiation,[36] Fas,[24,37] and TNF-α.[38] In γ-irradiated U87-W E6 cells, ceramide was produced with increased A-SMase activity, but not increased N-SMase activity. However, significant ceramide formation and activation of A-SMase were not observed in radioresistant U87-LXSN cells expressing functional p53. Inhibition of γ-radiation-induced ceramide formation by an inhibitor of A-SMase, SR33557,[23,24] resulted in the suppression of apoptosis. In contrast, enhancement of ceramide formation by OE potentiated radiation-induced apoptotic cell death. These results indicate that ceramide produced by A-SMase activation plays a pivotal role during p53-independent radiation-induced glioma cell apoptosis. Recent studies[36,39–41] have implicated ceramide in radiation sensitivity. The production of ceramide was deficient in the radioresistant lymphoid cell line WEHI-231 OE, although wild-type WEHI-231 JM cells accumulated ceramide in response to X-irradiation and underwent apoptosis.[39] The necessity of A-SMase (ceramide producing enzyme) in radiation-induced ceramide formation has also been demonstrated in cells from A-SMase-deficient Niemann–Pick patients and from A-SMase-knockout mice.[36] In highly radiation-resistant LNCaP prostate cancer cells, γ-irradiation had no effect on ceramide production.[41] However, these cells can be sensitized to radiation-induced cell death by exogenous C_2-ceramide or TNF-α, which increases ceramide formation. The effects of ceramide are thought to be mediated by serine proteases, which trigger mitochondrial membrane depolarization and caspase-9 activation. These and our present results suggest that suppressed activation of A-SMase (ceramide-producing enzyme) and upregulation of acid ceramidase (ceramide-degrading enzyme), both of which inhibit ceramide accumulation, are involved in radioresistance of glioma cells with endogenous functional p53. Significant radiation-induced activation of A-SMase was observed in neither U87-LXSN nor U87-M E6 cells expressing functional p53. Although no upstream regulator of A-SMase has been identified yet, our results implicate p53 in the blockage of A-SMase. The substances involved in and the processes of radiation-induced activation of A-SMase will be the subject of future investigation. To our knowledge, we have, for the first time, demonstrated upregulation of acid ceramidase in response to γ-radiation. Its increase was more prominent in glioma cells possessing endogenous functional p53 than in cells depleted of p53 by HPV-16 E6 protein. Therefore, p53 may play a role in the expression of acid ceramidase. OE, which is often used to inhibit ceramidase activity,[6,25,26] unexpectedly, downregulated radiation-induced expression of acid ceramidase. This drug accelerated radiation-induced apoptosis of U87-W E6 cells through enhanced accumulation of ceramide. Moreover, radioresistant U87-LXSN and U87-M

E6 cells can be sensitized to radiation-induced cell death by OE. Ceramide degradation is the only catabolic source of intracellular sphingosine.[42] Acid ceramidase activity may be the rate-limiting step in determining the intracellular levels of sphingosine, and subsequently, sphingosine-1-phosphate (SPP), an inducer of proliferation and survival.[43,44] Therefore, ceramidase plays a crucial role in the determination of ceramide/SPP ratio and, consequently, in cell survival or cell death in response to external stimuli.

In summary, ceramide generated through the activation of A-SMase, but not N-SMase, triggers γ-radiation-induced apoptosis in human glioma cells without functional p53, and that endogenous wild-type p53 eliminates the ceramide signal through upregulating acid ceramidase and blockade of A-SMase, and then protects glioma cells from γ-radiation-induced apoptosis. Further studies are necessary to clarify the relationship between p53 status and radiation sensitivity. Elucidation of the roles of p53 in ceramide metabolism (both production and elimination) may provide an insight into the development of γ-radiation therapy for malignant brain tumor.

Materials and Methods

Reagents

Dulbecco's modified Eagle's medium (DMEM) was purchased from Nipro (Osaka, Japan). Penicillin/ streptomycin was from Gibco-BRL (Grand Island, NY, USA). Fetal bovine serum (FBS) was from Irvine Scientific (Santa Ana, CA, USA). Gateway adaptor PCR system, pDONR221, BP clonase, and LR clonase were from Invitrogen (Tokyo, Japan). MTT, OE, and *E. coli* diacylglycerol kinase were obtained from Sigma (St. Louis, MO, USA). Immobilon-P membranes were from Millipore (Bedford, MA, USA). A protease inhibitor E-64 was obtained from Peptide Institute (Osaka, Japan). [γ-^{32}P]ATP and ECL Western blotting detection reagents were from Amersham (Buckinghamshire, UK). [1-^{14}C]Palmitic acid (55.0 mCi/mmol) was from ICN (Irvine, CA, USA). [choline-methyl-^{14}C]SM (52.0 mCi/mmol) was from NEC Life Science Products (Boston, MA, USA). High-performance thin-layer chromatography (HPTLC) plates were from Merck (Darmstadt, Germany). SR33557 was kindly supplied by Dr. Jean-Marc Herbert (Sanofi-Synthelabo Recherche, France). The primary antibodies used were anti-p53 monoclonal antibody (Ab-6) (Calbiochem-Novabiochem International, Boston, MA, USA), anti-acid ceramidase monoclonal antibody (Transduction Laboratories, Lexington, KY, USA), anti-p21^{WAF1} polyclonal antibody (Santa Cruz Biotechnology, CA, USA), anti-GADD45 polyclonal antibody (Santa Cruz Biotechnology), and anti-actin monoclonal antibody (Calbiochem-Novabiochem International). BCA protein assay reagents were obtained from Pierce (Rockford, IL, USA). Other chemicals were of the highest quality available.

Cell culture and stimulation

The human U-87 MG glioblastoma cell lines were obtained from American Type Culture Collection (Rockville, MD, USA). U87-LXSN, U87-W E6, and U87-M E6 cell lines were obtained by infecting U-87 MG cells with LXSN, LXSN-16E6SD, and LXSN-16E6SD-8S9A10 T retroviruses, respectively, followed by drug selection with 800 μg/ml G418 for 2 weeks.[8] p53 was also targeted by siRNA using retroviral delivery of shRNA. To generate retrovirus vector expressing shRNA, the self-inactivating virus vector was used. The 3'-LTR in a murine stem cell virus vector, pCMSCVpuro-DEST,[45] was inactivated by an internal deletion (*NheI-XbaI*). The self-inactivating virus vector was named pSI-CMSCVpuro-DEST. The H1 promoter cassette with or without stuffer previously described by Brummelkamp *et al*.[21] was attached by attB2 and attB1 sequences by adaptor PCR, and recombined into pDONR221 by BP reaction according to the manufacturer's instruction to generate pENTR221-H1R-stuffer or pENTR-H1R. To generate pENTR221-H1Rp53Ri, the pENTR221-H1R-stuffer was digested with *BglI* and *HindIII*, and the annealed oligos (5'gatccccGACTCCAGTGGTAATCTACttcaagagaGTAGATTGAGTCttttt-Ctttttggaaa3' and 5'agcttttccaaaaaGACTCCAGTGGTAATCTACtctc-ACtctcttgaaGTAGCTGGAGTCgggg3')[21] were replaced with the stuffer. Both the inserts were recombined into pSI-CMSCVpuro-DEST by LR reaction according to the manufacturer's instruction to generate pSI-CMSCVpuro-H1R-p53Ri and pSI-CMSCVpuro-H1R. U-87 MG cells expressing p53 shRNA (designed as U87-p53SI) and the control cells H1R (U87-Vec) were obtained by infection of SI-MSCVpuro-H1R-p53Ri and the backbone (SI-MSCVpuro-H1R) retroviruses, respectively, followed by selection with 1 μg/ml of puromycin. The cells were maintained in DMEM supplemented with 10% (v/v) FBS, 100 U/ml penicillin, and 100 μg/ml streptomycin (FBS/DMEM) in a humidified atmosphere containing 5% CO_2 at 37°C. Prior to γ-radiation, the cells were plated at a density of 1 $\times$ 10^4/ml and cultured for 3 days. Cells were irradiated using a ^{137}Cs source (IBL 437C Irradiator, CIS bio international, Gif-sur-Yvette, France) at a dose rate of 6.0 Gy/min.

Determination of apoptosis

Apoptotic cells stained with Hoechst 33258 were quantified by fluorescent microscopic analysis.[33] Briefly, cells were fixed in 1% glutaraldehyde for 30 min. The cells were then stained with 10 μM Hoechst 33258 for 10 min. Nuclear morphology was observed under a fluorescent microscope (Olympus BX60, Tokyo, Japan). For MTT assay, 500 cells were plated in 96-well microplates in 100 μl FBS/DMEM and cultured for 2 days prior to irradiation. At 3 days after γ-radiation, 50 μl MTT reagent (5 mg/ml in phosphate-buffered saline, PBS) was added to each well. After incubation at 37°C for 2 h, MTT was removed from the well, and the MTT formazon product was dissolved in 100 μl of dimethyl sulfoxide. The absorbance of the sample at 560 nm was measured using a microplate reader (Immuno Mini NJ2300, System Instruments, Tokyo, Japan).

Colony formation assay

U87-LXSN, U87-M E6, and U87-W E6 cells were irradiated at various doses, and cultured for 3 days. The cells treated with γ-radiation were washed with PBS and trypsinized. All the groups were replated at a density of 3000 cells/100 mm Petri dish in triplicate, and incubated for 2 weeks to allow colonies to develop. After 2 weeks, the medium was removed and the colonies were washed once with PBS, and fixed with 75% methanol in 25% acetic acid for 5 min and then the plates were dried. Colonies were stained with trypan blue in 50% ethanol for 10 min and subsequently washed with deionized water to remove excess dye.

SMase assay

Membrane fraction was prepared as described previously.[6,24] The activities of both N- and A-SMases were determined using a mixed micelle assay system.[6–8] For measuring N-SMase activity, the membrane fractions (20 μg protein) were mixed with [*choline-methyl*-^{14}C]SM (40 000 c.p.m. in 1 nmol of bovine brain SM in 0.25% Triton X-100 solubilized by sonication) in 0.1 M Tris/HCl buffer (pH 7.4) containing 6 mM $MgCl_2$, and the reaction mixture was incubated for 30 min at 37°C.

A-SMase activity in the membrane was measured as above, except that the Tris/HCl buffer was replaced with 0.1 M sodium acetate buffer (pH 5.5) containing 5 mM EDTA.

Measurement of cellular ceramide

Lipids extracted from cells were first treated in 0.1 M KOH in chloroform : methanol (1 : 2, v/v) at 37°C for 1 h.[6,33] Ceramide was converted to ceramide 1-[^{32}P]phosphate by *E. coli* diacylglycerol kinase in the presence of [γ-^{32}P]ATP,[6,33] and then lipids were separated on HPTLC plates in a solvent system of chloroform : acetone : methanol : acetic acid : water (50 : 20 : 15 : 10 : 5, v/v). Following autoradiography, spots corresponding to ceramide 1-phosphate were scraped into vials and the radioactivity was counted in a scintillation counter (Beckman LS-6500). Quantitation of ceramide was based on a standard curve of known amounts of ceramide. The changes in ceramide content were normalized based on total protein. The changes of cellular ceramide levels were also analyzed in cells labeled with [^{14}C]palmitic acid.[6,33] To radiolabel sphingolipids, cells were labeled with [^{14}C]palmitic acid (1 μCi/ml) for 24 h. The changes in [^{14}C]ceramide were normalized based on 100 μg of protein.

Western blot analysis

Cells were solubilized with ice-cold lysis buffer containing 1% Triton X-100, 50 mM NaCl, 25 mM HEPES (pH 7.4), 1 mM EDTA, 1 mM phenylmethylsulfonyl fluoride, and 10 μg/ml E-64. Extracted proteins (60 μg/well) were separated by sodium dodecylsulfate polyacrylamide gel electrophoresis (SDS-PAGE) on 6, 10, or 13% polyacrylamide gels, and were electrophoretically transferred onto Immobilon-P membrane. Blocking was performed in Tris-buffered saline containing 5% skimmed-milk powder and 0.1% Tween-20. The membranes were probed with antibodies against acid ceramidase and actin. Detection was performed with ECL system. Protein content was determined with BCA protein assay using bovine serum albumin as a standard.

Statistical analysis

Data are expressed as means $\pm$ S.D. Significance was assessed by two-way ANOVA, followed by Scheffe's *post hoc* test. *P*-values less than 0.01 were considered as significant.

Acknowledgements

We are grateful to Jean-Marc Herbert (Sanofi-Synthelabo Recherche, France) for SR33557. This work was supported in part by Grants-in-Aid for Scientific Research (B) (14370429) and Cancer Research (14026065) from The Ministry of Education, Culture, Sports, Science and Technology of Japan. M Sawada is a Research Fellow of the Japan Society for the Promotion of Science.

References

1. Sheline GE (1977) Radiation therapy of brain tumors. Cancer 39: 873–881
2. Taghian A, Suit H, Pardo F, Gioioso D, Tomkinson K, DuBois W and Gerweck L (1992) *In vitro* intrinsic radiation sensitivity of glioblastoma multiforme. Int. J. Radiat. Oncol. Biol. Phys. 23: 55–62
3. Sellers WR and Fisher DE (1999) Apoptosis and cancer drug targeting. J. Clin. Invest. 104: 1655–1661
4. Wolf BB and Green DR (1999) Suicidal tendencies: apoptotic cell death by caspase family proteinases. J. Biol. Chem. 274: 20049–20052
5. Hannun YA (1996) Functions of ceramide coordinating cellular responses to stress. Science 274: 1855–1859
6. Sawada M, Nakashima S, Banno Y, Yamakawa H, Hayashi K, Takenaka K, Nishimura Y, Sakai N and Nozawa Y (2000) Ordering of ceramide formation, caspase activation, and Bax/Bcl-2 expression during etoposide-induced apoptosis in C6 glioma cells. Cell Death Differ. 7: 761–772
7. Sawada M, Nakashima S, Banno Y, Yamakawa H, Takenaka K, Shinoda J, Nishimura Y, Sakai N and Nozawa Y (2000) Influence of Bax or Bcl-2 overexpression on the ceramide-dependent apoptotic pathway in glioma cells. Oncogene 19: 3508–3520
8. Sawada M, Nakashima S, Kiyono T, Nakagawa M, Yamada J, Yamakawa H, Banno Y, Shinoda J, Nishimura Y, Nozawa Y and Sakai N (2001) p53 regulates ceramide formation by neutral sphingomyelinase through reactive oxygen species in human glioma cells. Oncogene 20: 1368–1378
9. Waldman T, Zhang Y, Dillehay L, Yu J, Kinzler K, Vogelstein B and Williams J (1997) Cell-cycle arrest versus cell death in cancer therapy. Nat. Med. 3: 1034–1036
10. El-Deiry WS (1998) Regulation of p53 downstream genes. Semin. Cancer Biol. 8: 345–357
11. Moroni MC, Hickman ES, Denchi EL, Caprara G, Colli E, Cecconi F, Muller H and Helin K (2001) Apaf-1 is a transcriptional target for E2F and p53. Nat. Cell Biol. 3: 552–558
12. Dbaibo GS, Pushkareva MY, Rachid RA, Alter N, Smyth MJ, Obeid LM and Hannun YA (1998) p53-dependent ceramide response to genotoxic stress. J. Clin. Invest. 102: 329–339
13. Tepper AD, de Vries E, van Blitterswijk WJ and Borst J (1999) Ordering of ceramide formation, caspase activation, and mitochondrial changes during CD95– and DNA damage-induced apoptosis. J. Clin. Invest. 103: 971–978
14. Gomez-Manzano C, Fueyo J, Kyritsis AP, Steck PA, Roth JA, McDonnell TJ, Steck KD, Levine VA and Youg WKA (1996) Adenovirus-mediated transfer of the p53 gene produces rapid and generalized death of human glioma cells via apoptosis. Cancer Res. 56: 694–699
15. Lang FF, Yung WK, Raju U, Libunao F, Terry NH and Tofilon PJ (1998) Enhancement of radiosensitivity of wild-type p53 human glioma cells by adenovirus-mediated delivery of the *p53* gene. J. Neurosurg. 89: 125–132
16. Badie B, Goh CS, Klaver J, Herweijer H and Boothman DA (1999) Combined radiation and p53 gene therapy of malignant glioma cells. Cancer Gene Ther. 6: 155–162
17. Shono T, Tofilon PJ, Schaefer TS, Parikh D, Liu T-J and Lang FF (2002) Apoptosis induced by adenovirus-mediated *p53* gene transfer in human glioma correlates with site-specific phosphorylation. Cancer Res. 62: 1069–1076
18. Haas-Kogan DA, Yount G, Haas M, Levi D, Kogan SS, Hu L, Vidair C, Deen DF, Dewey WC and Israel MA (1996) p53-dependent G1 arrest and p53-independent apoptosis influence the radiobiologic response of glioblastoma. Int. J. Radiat. Oncol. Biol. Phys. 36: 95–103
19. Tada M, Matsumoto R, Iggo RD, Onimaru R, Shirato H, Sawamura Y and Shinohe Y (1998) Selective sensitivity to radiation of cerebral glioblastomas harboring p53 mutations. Cancer Res. 58: 1793–1797
20. Scheffner M, Huibregtse JM, Vierstra RD and Howley PM (1993) The HPV-16 E6 and E6-AP complex functions as a ubiquitin-protein ligase in the ubiquitination of p53. Cell 75: 495–505
21. Brummelkamp TR, Bernards R and Agami R (2002) A system for stable expression of short interfering RNAs in mammalian cells. Science 296: 550–553
22. Kiyono T, Foster SA, Koop JI, McDougall JK, Galloway DA and Klingelhutz AJ (1998) Both Rb/p16^{INK4a} inactivation and telomerase activity are required to immortalize human epithelial cells. Nature 396: 84–88
23. Jaffrezou JP, Levada T, Chatelain P and Laurent G (1992) Modulation of subcellular distribution of doxorubicin in multidrug resistant P388/ADR mouse leukemia cells by the chemosensitizer (2-isopropyl-1-(4-[3-*N*-methyl-*N*-(3,4-dimethoxy-β-phenethyl)amino]propyloxy)-benzenesulfonyl)indolizine. Cancer Res. 52: 6440–6446
24. Sawada M, Nakashima S, Kiyono T, Yamada J, Hara S, Nakagawa M, Shinoda J and Sakai N (2002) Acid sphingomyelinase activation requires caspase-8 but not p53 nor reactive oxygen species during Fas-induced apoptosis in human glioma cells. Exp. Cell Res. 273: 157–168